Effects of Roughness on Hypersonic Boundary-Layer Transition*

Steven P. Schneider†
School of Aeronautics and Astronautics
Purdue University
West Lafayette, IN 47907-1282

Abstract

The effect of roughness on hypersonic boundary-layer transition has been studied for three primary purposes: to trip a laminar layer to turbulence, to determine whether naturally occurring roughness is expected to cause early transition, and to determine the largest allowable roughness that will not affect the location of transition. Roughness is often divided into two classes: *isolated* roughness in which each protuberance can be considered separately, and *distributed* roughness similar to sandpaper, in which the roughness elements are many and are not considered separately. The effects of roughness on hypersonic transition are reviewed, considering the physics of the process, known parametric effects, some of the common correlations, and a few case studies. The three or more modes by which roughness can affect transition are outlined. At hypersonic edge Mach nunbers, it requires very large roughness heights to affect transition. Various correlations are often used to estimate the effect of roughness; several of these are described, although none provide good agreement with all the data.

Introduction

Brief Introduction to Hypersonic Transition

Laminar-turbulent transition in hypersonic boundary layers is important for prediction and control of heat transfer, skin friction, and other boundary layer properties. Vehicles that spend extended periods at hypersonic speeds may be critically affected by the uncertainties in transition prediction, depending on their Reynolds numbers. However, the mechanisms leading to transition are still poorly understood, even in low-noise environments. These mechanisms include the concave-wall Görtler instability [1], the first and second mode streamwise-instability waves described by Mack [2], and the 3D crossflow instability [3, 4].

Many transition experiments have been carried out in conventional ground-testing facilities over the past 50 years [5]. However, these experiments are contaminated by the high levels of noise that radiate from the turbulent boundary layers normally present on the wind tunnel walls [6]. These noise levels, typically 0.5-1% of the mean, are an order of magnitude larger than those observed in flight [7, 8]. These high noise levels can cause transition to occur an order of magnitude earlier than in flight [6, 8]. In addition, the mechanisms of transition operational in small-disturbance environments can be changed or bypassed altogether in high-noise environments; such changes in the mechanisms usually change the parametric trends in transition [7]. Although transition can become completely dominated by roughness [9] or perhaps ablation effects, these effects are usually only one of several factors whose effect must be understood to reliably predict flight [7, 10]. Mechanism-based prediction methods must be developed, supported in part with measurements of the mechanisms in quiet wind tunnels.

Introduction to Roughness Effects

In most cases the effect of roughness is to move transition forwards, with the amount of forward movement increasing with roughness height. A classical example is shown in Fig. 1, which also serves to define some basic terminology. The figure is redrawn from Fig. 12 in Ref. [11], and the Mach number at the boundary-layer edge was $M_e = 1.9$. Van Driest and McCauley measured transition due to an azimuthal row of spherical roughness elements, on a 5-deg. half-angle sharp cone at zero angle of attack, in the 12-inch supersonic wind tunnel at the Jet Propulsion Laboratory [11]. The freestream Mach

*AIAA-2007-0305, presented at the Jan. 2007 AIAA Aerospace Sciences Meeting

†Professor. Associate Fellow, AIAA.

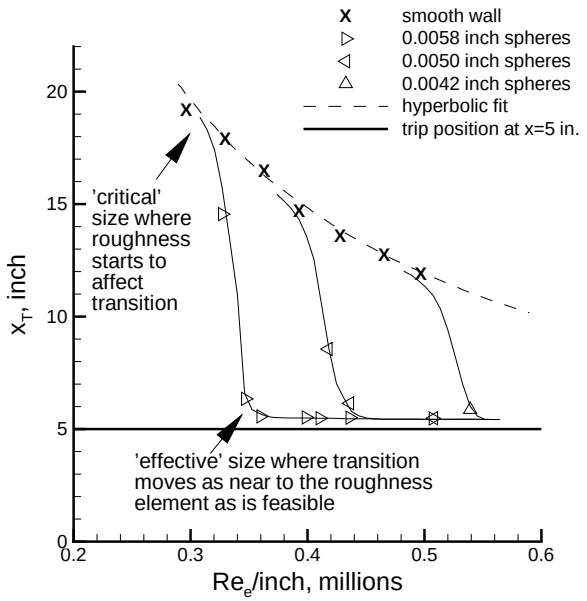

Figure 1: Definition of Critical and Effective Roughness

number was varied from 1.97 to 3.84 by varying the flexible-plate nozzle.

Ref. [11] gives the smooth-wall transition Reynolds number as $Re_0 = 5.9 \times 10^6$, based on arclength to the end of transition and on edge conditions. The hyperbolic fit to the smooth-wall data, shown in Fig. 1, shows that this transition Reynolds number was approximately independent of unit Reynolds number, which in light of later research is at first somewhat surprising [7]. However, at higher Mach number the transition Reynolds number becomes dependent on unit Reynolds number, as might be expected, given the rapid increase in the noise radiated from the nozzle-wall turbulent boundary layer (which Van Driest and McCauley were not yet aware of). At the higher Mach numbers, the transition Reynolds number is lower at lower unit Reynolds numbers, as is typical. The smooth-wall transition Reynolds number decreases with Mach number, from about 5.9×10^6 at $M_\infty = 1.97$ to about 3.4×10^6 at $M_\infty = 3.84$; again, this is presumably due to the increase in tunnel noise. It would be interesting to compare these values to Pate's correlation [12].

When a relatively large roughness of 0.0058 in. is applied, the forward movement of transition with unit Reynolds number begins to depart from the smooth-wall value at about $Re_e \simeq 0.3 \times 10^6$/in. Here, Re_e is a unit Reynolds number based on conditions at the boundary-layer edge. This initial departure from the smooth-wall data defines the *'critical'* conditions for the roughness, where it first begins to have an effect. As the unit Reynolds number is increased further, the boundary-layer thickness continues to decrease, the roughness appears larger to the flow, and the roughness-induced transition moves forward much more rapidly than the smooth-wall transition. Note that the solid lines in Fig. 1 were apparently hand-faired by Van Driest and McCauley without explanation, to guide the reader. This rapid movement is a common indicator for roughness effects, but does not always occur. When Re_e reaches about 0.35×10^6/in. for the 0.0058-in. roughness, the transition location has reached nearly to the roughness element, although not quite all the way to the roughness element itself. For this condition the roughness is termed *'effective'*, in the sense that the roughness is tripping the boundary layer as effectively as possible, and further increases in roughness height only provide larger disturbances to the flow, without moving transition any farther forward. Smaller roughness has a similar effect at higher unit Reynolds numbers when the boundary layer is thinner.

For Fig. 1, a single row of spherical roughness elements are placed spanwise around the azimuth at the 5-inch station. Transition was detected using azobenzene in the region near the roughness elements, magnified Schlieren for regions farther downstream, and thermocouples for regions yet farther downstream. Fig. 2, scanned from Fig. 10a in Ref. [11], shows an azo-benzene surface sublimation image, obtained at $M_e = 3.67, x_k = 5$ in., and an unspecified Reynolds number. The spherical trips of height 0.015 in. are visible on the cone; they are spaced 1/32 in. apart. Transition is taken to occur at the location where the streaks behind the trips in the azobenzene begin to widen and 'contaminate' the laminar-flow to the side. Transition is attributed to the breakdown of spiral vortices shed from each side of the roughness element. The vortical streaks persist into the turbulent region.

Fig. 3, scanned from Fig. 8 in Ref. [11], shows roughness-induced transition on the cone as measured with three different techniques, at three different unit Reynolds numbers. The upper row of photos are Schlieren images, magnified in the wall-normal direction, to make visible the transition-induced increase in boundary-layer growth rate. The middle row of images are from azo-benzene surface sublimation; the streamwise location of the roughness array is indicated, along with the streamwise lo-

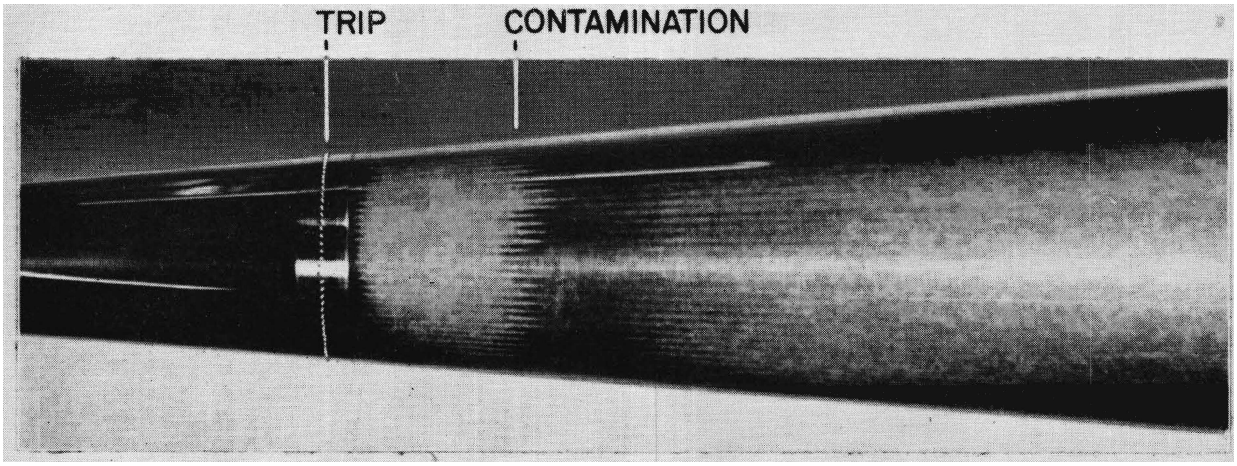

Figure 2: Surface Flow Visualization of the Roughness-Induced Transition Process

cation at which the roughness wakes begin to spread, indicating transition. Once the vortices break down to turbulence, the turbulence grows spanwise within fan-shaped regions that eventually merge. Transition is indicated at a similar streamwise location in both the Schlieren and azo-benzene images (see also Ref. [13] for a comparison of different methods of inferring the onset and end of transition). The lower row of graphs plots the adiabatic wall temperature divided by the temperature at the boundary-layer edge; this rises even ahead of the trip location, due to axial conduction within the skin. Aft of the trip location, the wall temperature rises in part due to transition and in part due to heating from the vorticity in the wake of the roughness. The peak in the surface temperature is near the transition location indicated by the imaging techniques; however, it is difficult to give the locations of the onset and end of transition.

Van Driest and Blumer show a figure similar to Fig. 1 in a later paper [14]. By design, the roughness elements were generally placed so as to induce transition *'sufficiently far forward of the smooth wall transition – i.e., sufficiently far forward of transition induced by free-stream disturbances.'* These measurements were all carried out at $M_e = 2.71$, using a 5-deg. half-angle sharp cone in the 12-inch supersonic tunnel at JPL. Transition was detected via Schlieren images which were magnified in the wall-normal direction. Fig. 4 shows their definition of terms, redrawn from their Fig. 4, and updated from Fig. 1. The horizontal axis is the unit Reynolds number at the boundary layer edge, and the vertical axis is the distance along the surface of the cone from the apex to the location of transition. The transition location when the cone is smooth is shown as curve 4. *'When a ring of spherical elements of size k is placed at position x_k, the movement of transition takes the course indicated by curves 1, 2, and 3 successively as the unit Reynolds number is increased. The relative roles played by disturbances from the roughness elements and the free stream are readily indicated. In zone 1, the free-stream disturbances are predominant in establishing transition, whereas in zone 3 the roughness element predominates in locating transition. In zone 2, the roughness element has become large enough relative to the boundary-layer thickness to produce a drastic forward movement of transition, however, the effect of free-stream disturbances must still be considered in this region.'*

Van Driest and Blumer further clarify this behavior by plotting 14 figures showing the variation of transition Reynolds number (Re_t) with roughness Reynolds number (Re_k) for varying nondimensional trip locations (x_k/k,) bringing up the importance of trip location, even for a sharp cone [14]. Here, x_k is the distance along the surface from the apex to the roughness location, Re_t is based on edge conditions and the arclength to transition, k is the roughness height, and Re_k is a Reynolds number based on k and conditions in the undisturbed laminar boundary layer at the roughness height. Figs. 5 and 6, redrawn from their Figs. 5c and 5m, show two samples. In both cases, the roughness Reynolds number is varied for a fixed roughness by varying freestream Reynolds number. The variation of the smooth-wall transition location is shown, for comparison. Both figures show that there is *'no appreciable effect of free-stream disturbances on the effective transition Reynolds number,'* although there is a small effect

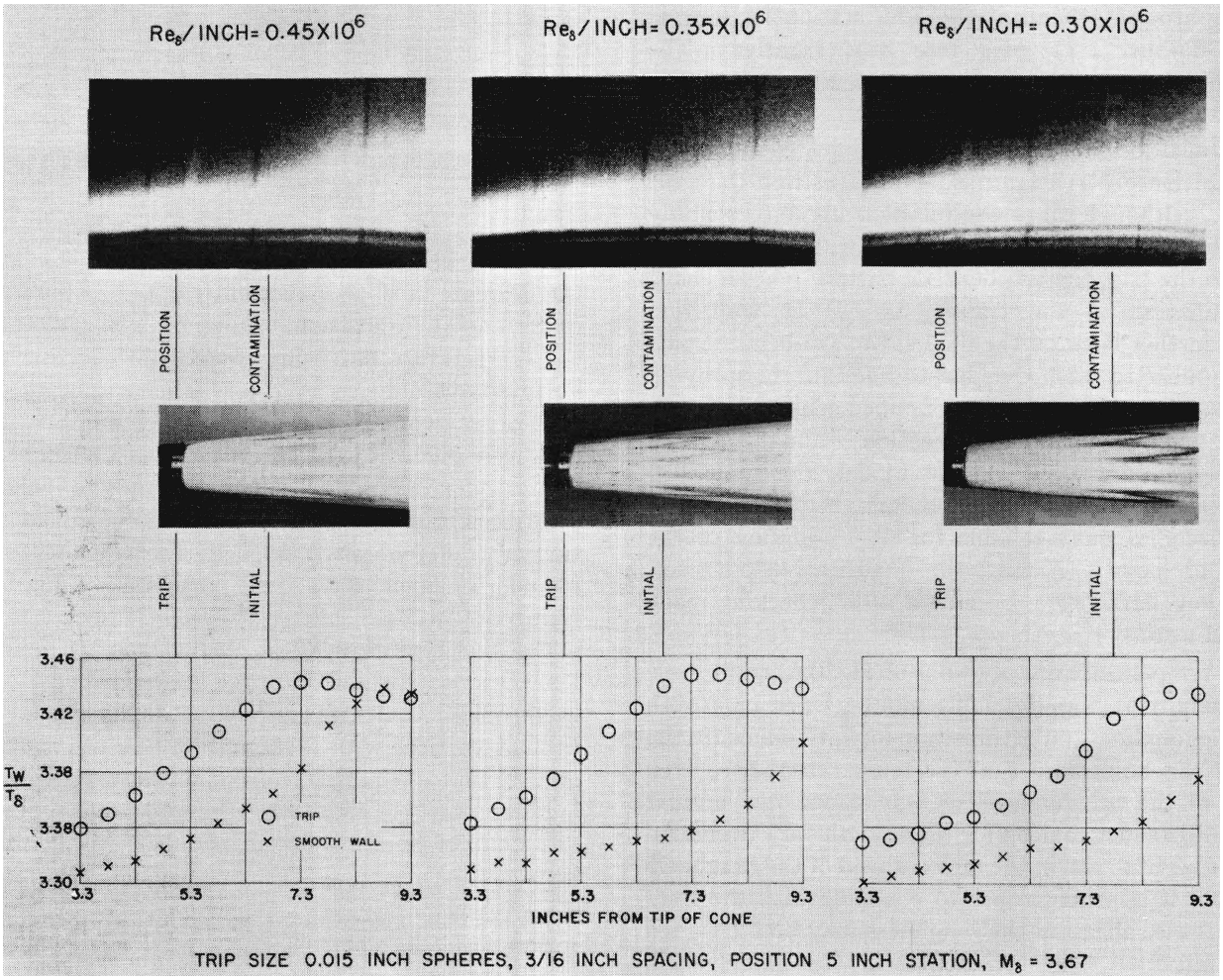

Figure 3: Comparison of Transition Due to Controlled Roughness by Magnified Schlieren, Azo-Benzene Patterns, and Temperature Distributions on a 5-deg. Half-Angle Cone

in Fig. 6. Van Driest and Blumer also identified two trends with x_k/k. In zone 1, for large x_k/k (Fig. 6), they found a region where the transition Reynolds number tracked the smooth-wall value, even when the roughness was present, while such a region was not present for smaller values of x_k/k. Apparently these roughness values were smaller than the 'critical' value necessary to affect transition. In addition, in zone 3, for small values of x_k/k (Fig. 5), an inflection or hump occurred near $Re_k = 3000$, with the size of the inflection decreasing with increasing x_k/k. This hump has never been explained.

Plotting the variation of transition Reynolds number with unit Reynolds number is generally a very instructive way to understand roughness effects, particularly when the smooth-wall transition location is also shown. However, this takes substantial experimental effort. In addition, much of the value is only available for sharp cones and flat plates, where the flow is self-similar with distance from the leading edge. For complex flows on 3D geometries, multiple models with differing scale would be necessary to more fully determine the effects of the roughness scale, and the additional expense has so far precluded this approach.

Roughness Effects at Lower Speeds

Since the effect of roughness at lower speeds is easier to measure and simulate, much more is known about it. This knowledge of low-speed roughness effects is critical background for an understanding of high-speed roughness effects. However, including the low-speed work would broaden the present review beyond a manageable scope. Some of the critical background may be found in Refs. [15], [16], [17], [18], [19], [20], [21], [22], [23], and [24].

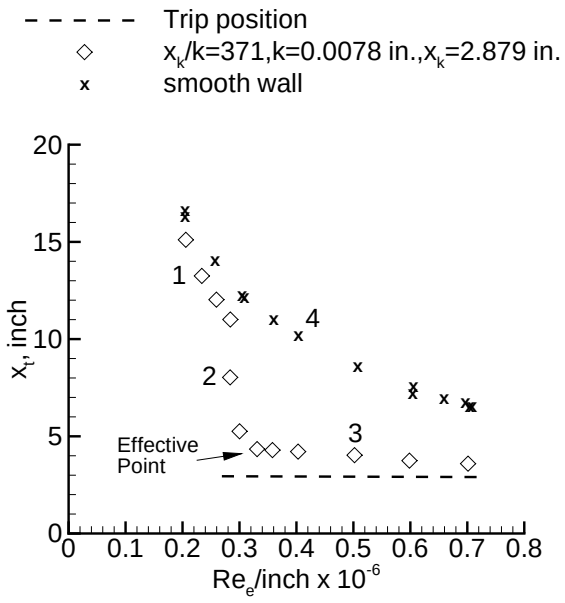

Figure 4: Variation of Transition Location with Unit Reynolds Number on a Cone at $M_e = 2.71$

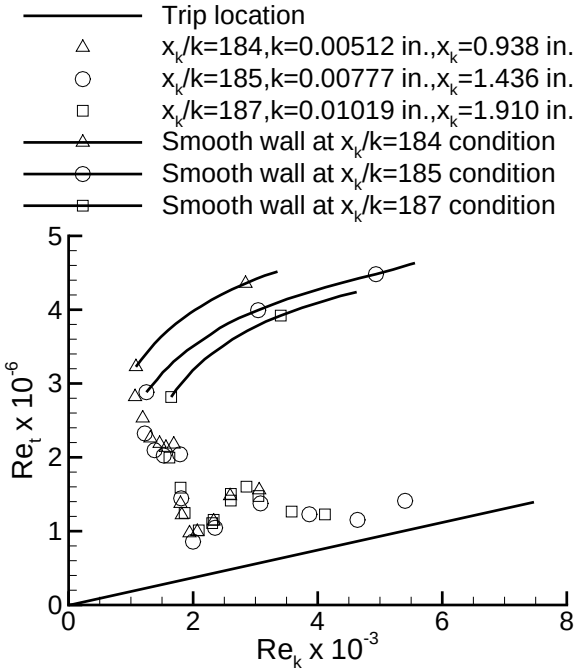

Figure 5: Variation of Transition Reynolds Number with Trip Reynolds Number on a Cone. Upstream Trips

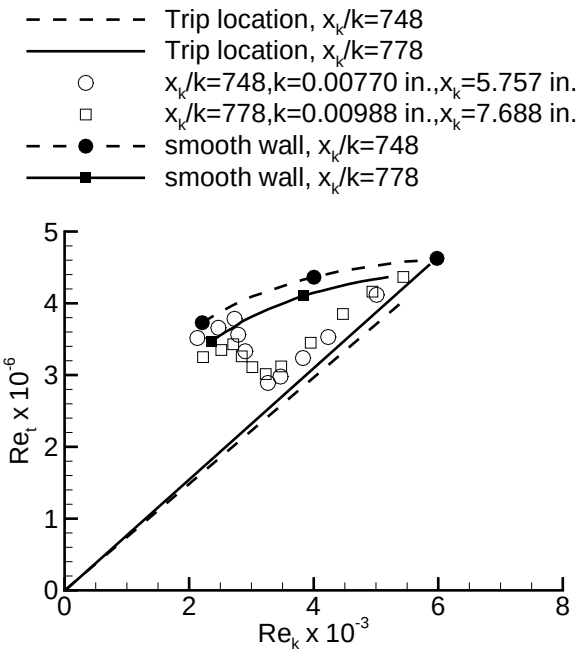

Figure 6: Variation of Transition Reynolds Number with Trip Reynolds Number on a Cone. Downstream Trips

Previous Reviews of Hypersonic Roughness Effects

Several reviews of the effects of roughness have been reported over the decades. Tani provided an overview of transition physics in Ref. [25] which includes issues related to roughness and hypersonics. Braslow reviewed early studies of distributed roughness effects in 1960 [26].

Tetervin reviewed the effects of instability and roughness on seven early flight tests of nominally-axisymmetric blunt vehicles [27]. Tetervin provided computations of instability and Re_k using early momentum-integral methods. Transition during the seven flights is more readily explained by roughness than by instability, although the computed values of Re_k are all less than 60, and in some cases less than 1. Tetervin provides extensive tabulations that might be useful if these flights were to be reanalyzed.

Wool reports a summary of the PANT program to estimate the onset of transition on the ablating hemispherical nosetips of sphere-cone reentry vehicles [28]. This Passive Nosetip Technology program was funded by the Space and Missile Systems Organization during 1971 to 1975 to aid in understanding and designing the carbon-composite nosetips for intercontinental ballistic missiles. Although much of this work is still not in the public domain, much has

been released. The PANT program focused on transition on the nosetip itself, in the subsonic region, so although the overall flowfield is hypersonic, $M_e < 1$. Wool's summary lists 23 volumes of PANT reports.

Work continued in this area of nosetip transition, leading to the 1981 reviews of Reda [29] and Batt and Legner [30]. These two authors propose different methods of correlating nearly the same data; they continued to disagree on the proper approach all the way to Dick Batt's death in August 2003, thereby illustrating the complexity and controversy that often surrounds this topic. Finson also reviewed the data and physics of this problem, considering several correlations [31]. Finson argues that his correlation and those of PANT and Van Driest all give similar predictions for flight conditions, while Bishop's criterion predicts higher transition Reynolds numbers [32].

Bishop reviewed roughness-induced transition on supersonic blunt bodies [33, 34]. He uses two different correlations, one near the stagnation point where the external streamlines have concave curvature, and another on the rest of the nosetip. For measurements at least 20-deg. from the stagnation point, Bishop correlates a fairly broad dataset with

$$\frac{Re_\theta}{\left[1 + 4.5\frac{T_w}{T_e}M_e^2\right]^{1/2}} = 5.6\left(\frac{k}{D}\right)^{-1/3}.$$

Here, D is the nosetip diameter, T_w is the wall temperature, T_e is the temperature at the boundary-layer edge, Re_θ is the Reynolds number based on edge conditions and momentum thickness, and M_e is the Mach number at the boundary-layer edge. The distribution of measured roughness is shown for ATJ-S graphite. Bishop believes that the largest roughness elements are the most important, and correlates using the height which is larger than 85% of the roughness distribution, k_{85}. The effects of wall temperature are large in Bishop's correlation, which is independent of tunnel noise. He finds no smooth-wall limit to the data, and includes some of the flight measurements on polished nosetips. Several of the plots in Bishop's public-release paper are drawn from references that are not in the public domain. The generality of Bishop's correlation is uncertain, but the paper appears to deserve further study. Ref. [34] provides a detailed tabulation of all the data analyzed.

Bertin reviews transition in his textbook on hypersonics, and includes 9 pages on roughness effects [35]. Transition on capsules and planetary probes was previously reviewed by the present author, without special attention to roughness effects [36]. Reda's 2002 review is discussed in a subsequent section describing the Re_k correlation [9].

Scope of the Present Review

The present author's personal library contains more than 200 papers discussing roughness effects on hypersonic or supersonic transition, and many others have certainly been published on this topic. Thus, the present review is certainly incomplete, and the author would appreciate having other articles drawn to his attention. It has been at least 25 years since the last comprehensive review of the literature in this area, for Reda's 2002 review [9] does not claim any comprehensive coverage of the literature.

A thorough review of this area would include the reanalysis of much of the existing data. There are many correlations that have been used in attempts to synthesize roughness-induced transition, and none of these correlations have ever been compared against a wide range of existing data in a comprehensive way. It would be very interesting and instructive to compare the accuracy and scatter of several of the most-common correlations against such a wide range of data. However, such a reanalysis would require extensive effort which was far beyond the scope of available resources.

To make the present review more tractable, an attempt has been made to limit it to hypersonic flows. However, this classification is in the eye of the beholder. When a vehicle or model is in a hypersonic freestream, the local flow near the surface has an edge Mach number that ranges from zero near the stagnation point to some larger value downstream. Few would argue that ICBM nose cones and the Space Shuttle are not hypersonic vehicles, yet the roughness on hypersonic sphere cones seems most important on the nosetip, where $M_e < 1$, and the edge Mach number on the windward centerline of the Shuttle rarely reaches above Mach 3. Thus, supersonic and even subsonic regions are considered as part of the present review, which nevertheless is focused on roughness effects thought to be important to hypersonic flows.

The literature for transition on blunt bodies with roughness and ablation is too large to include in the present review. A separate review of this literature is being developed in support of the Orion program [37]. Thus, the present review refers to this area only in passing.

Types of Roughness

Roughness can take many different forms. Roughness is usually thought of as either *'isolated'*

or *'distributed'*. Isolated roughness includes steps, gaps, joints, local flaws such as rivets and machining flaws, tripping elements, and so on. A major issue for hypersonic vehicles is often the actual condition of the heated and ablated vehicle surface, in flight prior to transition, including the actual thermal expansion effects, and the actual as-built surface, with all ports, inserts, and fasteners.

Distributed roughness might include sand-grain trips, screw threads, the patterns left on a metal surface by various machining and finishing processes, and the patterns generated on a thermal protection system by ablation. In principal, a nearly-infinite number of parameters would be needed to fully describe the detailed irregularities in a surface with distributed roughness. Future research thus needs to determine the parameters necessary to describe the critical features of a surface roughness for particular conditions, with these critical parameters likely to include some sort of Fourier analysis, for distributed roughness (see, for example, Ref. [38]).

The tiled surface of the space shuttle is an intermediate form; the myriad small tile-to-tile variations in surface contour might be considered distributed roughness, when examined from afar, or as isolated roughness, if the largest local flaws are examined in detail. The interaction of the effect of the various elements in a distributed roughness has not been studied much. Here, more attention is paid to isolated roughness elements, since more of the experimental work was carried out with this type. A comprehensive understanding of the various types of roughness effects remains a topic for future research.

It is helpful to have a general concept of the types of roughness likely to be present in flight; of course, these depend on the design of the thermal protection system, and on the way it is flown. Fig. 7, taken from Fig. 2 in Ref. [39], shows micrographs of polished cross-sections of several thermal protection materials that were ablated under laminar flow in an arc-jet. Three materials are shown, after an unspecified laminar ablation in an arcjet, which was sufficient to remove the original machined surface: CMT is a graphite material, but the acronym is not explained, FWPF is a Fine-Weave Pierced Fabric carbon/carbon composite, and '223 C/C' is 223 Carbon/Carbon. Each material leaves a different pattern and surface roughness when ablated. The magnification in the original document is shown along with the material type.

Fig. 8, taken from Fig. 1 in Ref. [40], and labeled as Manned Spacecraft Center photo S-66-22150, shows an image of an Apollo heat shield taken

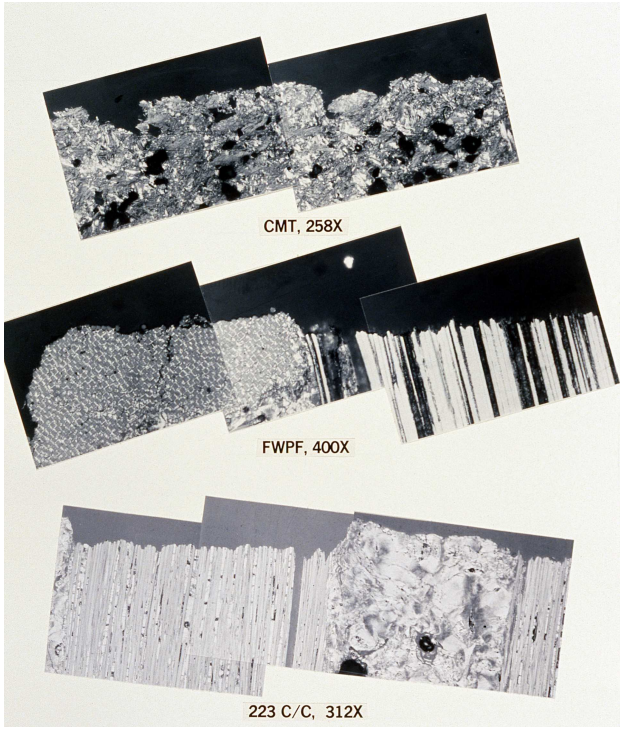

Figure 7: Cross-Sectional Views of Laminar-Ablated Surfaces

immediately after a qualification flight test, while the capsule is being lowered onto the deck. Per a caption forwarded from Mary Wilkerson in the Still Imagery Repository at NASA JSC, this is from unmanned mission AS-201 on 26 Feb. 1966. The irregular roughness due to ablation is evident, although this spacecraft probably ablated turbulent before the image was obtained. These images should provide some idea of the complexity of ablated surfaces.

Wilkins and Darsow reviewed the types of roughness normally present on ballistics-range models, and the properties of the different instruments used in 1959 to measure surface roughness [41]. The pros and cons of interferometry, profilometers, and optical sections are compared.

Physical Effects of Roughness

Most studies of the effect of roughness on transition have measured only the transition location and the roughness properties, as part of efforts to develop engineering correlations. Prior to the 1990's, numerical capabilities were insufficient to compute many details of the flowfields anyway. Klebanoff and Tidstrom carried out a pioneering study showing that wake instabilities could explain transition behind a

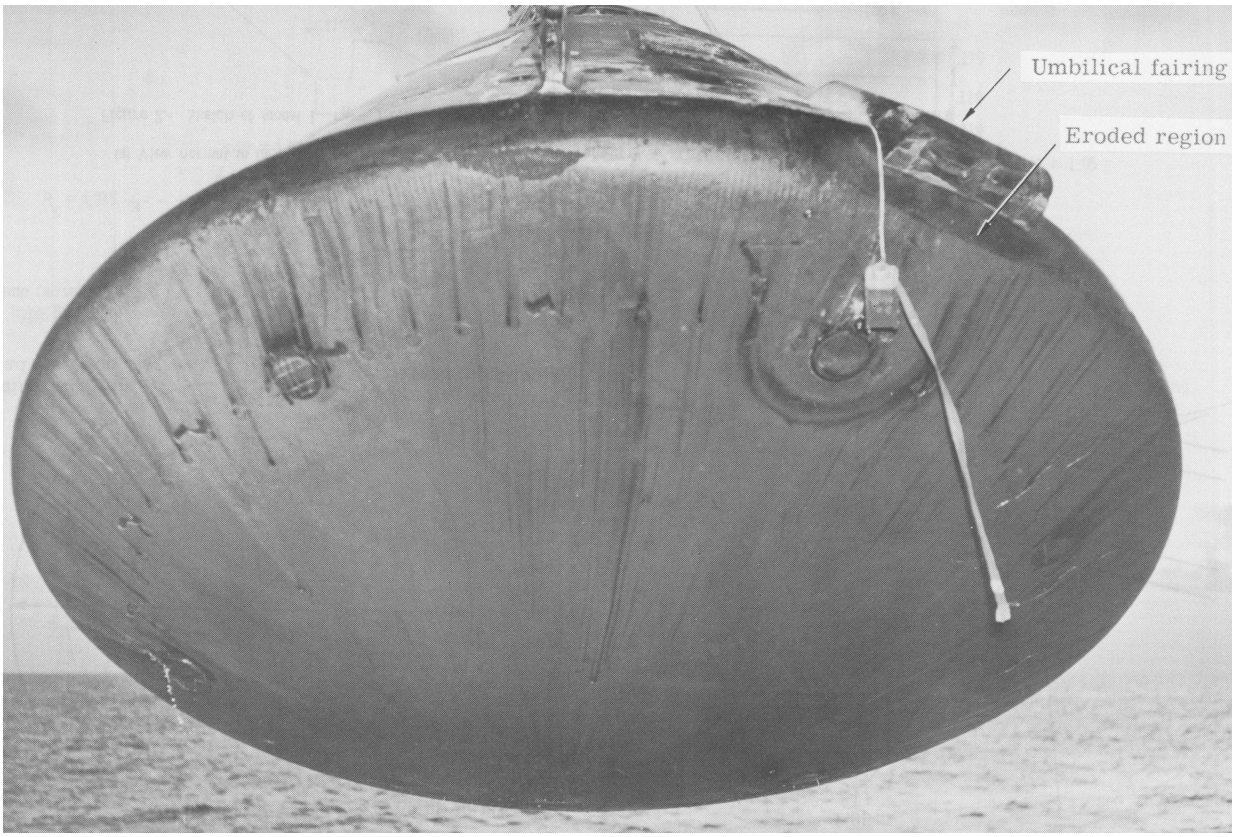

Figure 8: Apollo Heat Shield Immediately After Qualification Flight Test in Feb. 1966

2D roughness on a low-speed flat plate [42]. However, Klebanoff's computations were crude, even for this simple flow field.

However, a few studies have measured details of the roughness-induced flowfield, in attempts to develop a more detailed physical understanding of the process. At low speed, studies of the roughness-induced flowfields date back to the 1940's or earlier (see, for example, Ref. [43]). Morkovin reviewed studies of the physical mechanisms of roughness-induced transition at low speeds, in Ref. [44], for both 2D and isolated 3D roughness elements. Here, a brief and incomplete summary of some of the higher-speed work is made. Now that computations of such complex flowfields are almost routine, more of this work needs to be done.

Modes by which Roughness Can Affect Transition

There is no general mechanism-based theory for determining the conditions under which roughness can cause transition. There appear to be at least three fundamentally different ways by which roughness can affect instability and transition:

1. Roughness generates a wake with streamwise vorticity and a possibly unstable shear layer. This wake may transition to turbulence: either immediately, behind an 'effective' roughness, or farther downstream, behind a smaller roughness. The wake instability may be dominated by the instability of the shear layer or of the trailing vorticity; little is known about this problem at hypersonic speeds.

   Ergin and White recently reported very detailed hot-wire measurements of the wake behind isolated roughness elements at low speed on a flat plate; they also include a good review of the low-speed literature [24]. There, a good case is made that transition in the wake of an isolated roughness element *' . . . results from a race between unsteady fluctuation growth* [in the unstable wake] *and the rapid relaxation of the basic state toward a spanwise-uniform Blasius flow.'* This is probably a good way to think about the effect of isolated roughness elements, across all speed ranges.

   It appears that instabilities in the wake of the

roughness may depend on the nature of the roughness (2D or 3D, shape, height, etc.) and on the flowfield the roughness is placed in. Note that a high Mach number shear layer is less unstable [45, 46], which may explain the insensitivity of high Mach number flows to roughness effects. In many cases it appears that transition is dominated by the largest roughness elements, and there is little interaction among the roughnesses, unless they are too close together.

2. Streamwise vorticity behind small roughness elements ($Re_k < 10$) can grow via instability mechanisms such as stationary crossflow [23], Görtler [47], or transient growth [48]. These instabilities then lead to transition. In this case, the spanwise distribution of the roughness elements is often critical, along with the height and streamwise location. For swept wings at low speed, Saric's group has shown that carefully designed small roughness elements can even *delay* transition past the location where it would normally occur without them [3].

3. Roughness can interact with acoustic waves or other freestream disturbances to generate instability waves or precursors to instability waves via a receptivity process (see, for example, Refs. [49, 50, 51]). Spanwise and streamwise distribution is again important.

The present review focuses on the first of these three modes, which is the best known, although the physics of the process has not been studied much. For hypersonic flows, the latter two modes have not received much attention to date. The mechanism by which the roughness generates transition downstream appears to depend on model geometry and conditions.

Images of Surface Effects

Whitehead reported instructive oilflow images of the detailed flow near isolated roughness elements [52]. Whitehead's measurements were made on a 7.7-deg wedge in the Langley 11-inch hypersonic tunnel, at a freestream Mach number of 6.8. Fig. 9, taken from Fig. 4 in Ref. [52], shows detailed oilflow images of the surface flow near four kinds of elements. The edge Mach number is 5.5, the roughness height k is 2 times the boundary-layer thickness δ, and the element spacing s is eight times the element width w. The images appear to be at the same scale, and the diameter of the sphere is 0.238 cm. The boundary-layer thickness was obtained from a curve fit to pitot-probe measurements. *'The sketch shown for the sphere is typical of the flow field around these elements and shows several counterrotating vortex filaments which initiate ahead of the element and are forced downstream around the element, scouring the surface as they go.'*

The relationship between the boundary layer, the vortices, and the bow shock from the roughness element is unclear. It would be interesting to compare these oilflow data to a modern computation. The triangular prism is much less blunt, and the standoff distance for the vortices is also much less, suggesting there is a bow shock on the front of the roughness element that may play an important role in generating the vorticity. Shocks are regularly seen in Schlieren for roughness elements of heights comparable or larger than the boundary layer thickness, as here. The smaller standoff distance for the triangular element suggests a weaker shock and less trip drag.

Fig. 10, taken from Fig. 5a in Ref. [52], shows the effect of element spacing. The edge Mach number is 5.5, $k/\delta = 2$, $k = 0.238$ cm., and the elements are placed near the trailing edge of a 7.7-deg. wedge, as shown in the sketch. For s/w of 3-4 or more, the elements appear to act nearly independently, and transition occurs at nearly the same distance downstream of the element. When s/w is less than 3, transition occurs farther downstream, and the trips are less effective; Fig. 10 shows that in this case the trips are acting more like a fence than like individual vortex generators. At hypersonic speeds, at least on a flat plate, three-dimensional roughness induces earlier transition; the opposite is true at low speeds [42]. In Whitehead's Fig. 9, the drag per tripping element is shown to increase with trip spacing, all the way through $s/w = 20$, so it appears that the flowfields around the trips still do interact even for $s/w > 3$. The boundary layer clearly separates well forward of the trips; this is also visible in Fig. 9.

Fig. 11, taken from Fig. 7a in Ref. [52], shows an excellent oil-flow image of the downstream influence of large spherical roughness elements on a flat plate. The freestream and edge Mach numbers are 6.0, $k/\delta = 2$, and $s/w = 4$. The vortices generated near the roughness elements persist well downstream, apparently even into the turbulent region.

Fig. 12, taken from Fig. 7b in Ref. [52], shows the wake of a single roughness element as imaged using phase-change paint, which is sensitive to the heat transfer at the wall. The darker portions indicate regions of higher shear and temperature, thus showing the surface footprint of the vortices. The 5-

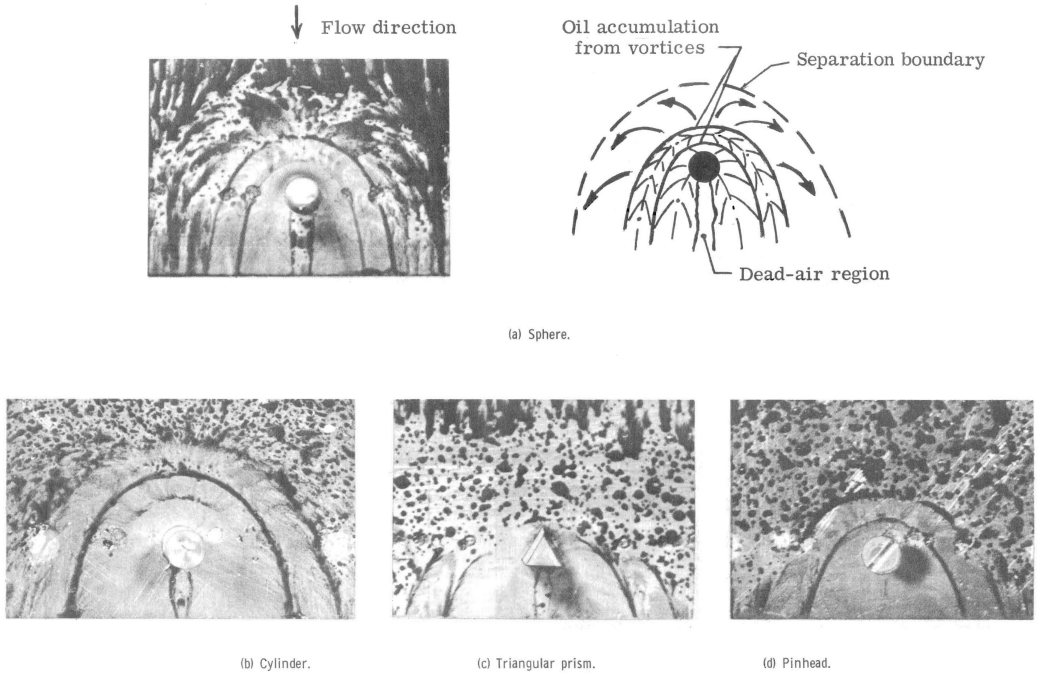

Figure 9: Flow Behavior Around Isolated Roughness Elements

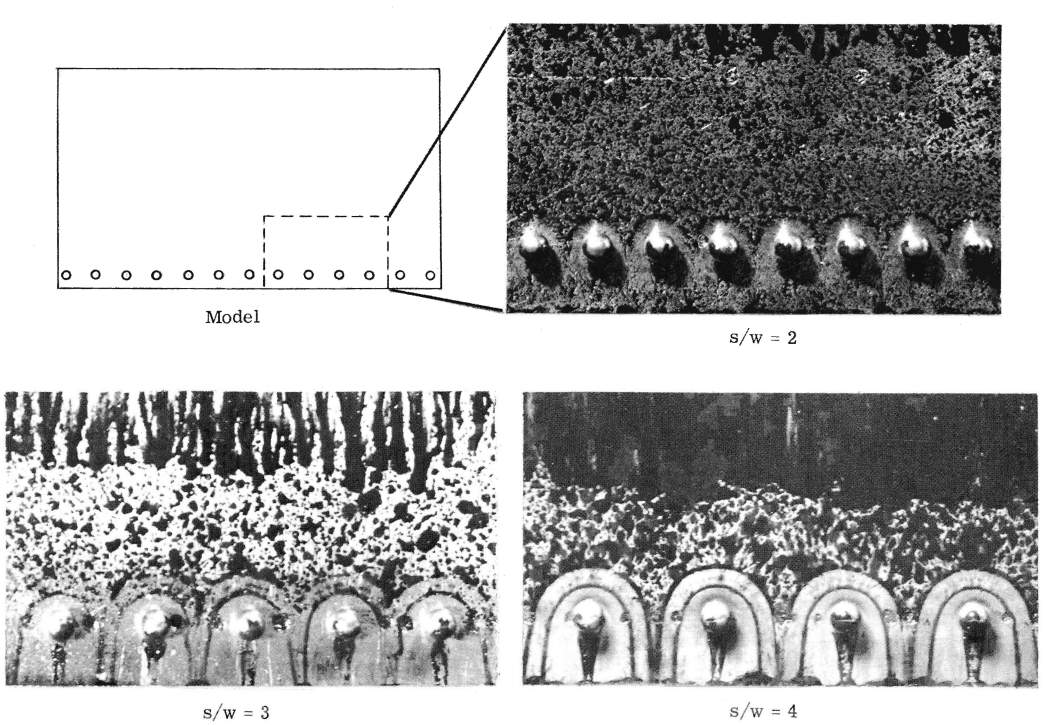

Figure 10: Effect of Spacing on Surface-Flow Patterns around Spherical Roughness Elements

deg. blunted cone was tested at a freestream Mach number of 8, with $k/\delta = 2.4$ and $s/w \simeq 2.8$.

These images were scanned in grayscale at 600 dots per inch, using an original printed copy of Ref. [52]. Unfortunately, the original photographs have been lost; although the report has numbered photographs which should be present in the NASA Langley photo archive, the numbers given don't correspond to the correct photos (Alicia Bagby, NASA Langley, private communication, October 2006). The quality of the photographs in the scanned documents presently provided by NASA STI is much reduced compared to the paper copy.

Braslow's Hypothesis: Re_k Should Scale Effects on Transition Only for Small Roughness

Braslow and Horton reviewed roughness effects on transition for subsonic and supersonic speeds [53]. Isolated roughness effects are only expected to scale with Re_k when the roughness height is much less than the boundary layer thickness: *'Good correlation using Re_k is expected whenever the roughness is well submerged in the boundary layer.'* For subsonic and low supersonic conditions, roughness of this height can still trip the boundary layer, presumably because the shear layers behind the roughness element are still subsonic. However, for hypersonic conditions, such roughness heights are no longer sufficient, presumably due to the increased stability of high-Mach shear layers [45, 46]. It would be interesting to see a clear test of this hypothesis.

Small Roughness Can *Delay* Transition

Although roughness usually acts to move transition forward, the opposite trend is possible. Holloway and Sterrett show that small roughness of 0.022 in. high on a sharp flat plate at Mach 6 actually *delays* transition onset from about 3.8 in. on a smooth plate to about 4.5 in. when roughness is added. The spanwise row of spherical elements was placed about 2.8 inches from the leading edge at $Re_e = 8.2 \times 10^6$/ft [54, Fig. 6f]. Similar results have been reported by others. The mechanism for the delay was unknown, and remains so.

Parametric Effects

Many factors influence the effect of roughness on transition, in addition to the obvious factors of roughness height, boundary-layer thickness, and Reynolds number. Some of these factors are explored in the following subsections.

The Influence of Roughness Shape

Whitehead also looked at the effectiveness of various shapes of isolated roughness, for tripping purposes [52]. The ideal roughness element trips the flow to turbulence very rapidly, without producing much drag at the roughness itself. Whitehead studied the usual spheres, along with triangular prisms, cylinders, pinheads, and two vortex-generator shapes. A vortex-generating fin had less drag for the same frontal area, suggesting it might improve on the usual spheres for tripping purposes, but Whitehead did not investigate the tripping effectiveness of the fin.

Hicks and Harper evaluated both the usual spherical trips and also triangular pieces of tape, with the point of the triangle facing into the flow [55]. The measurements were made on sharp flat plates in the Ames 1 by 3-ft. supersonic tunnel at freestream Mach numbers of 1.58, 2.17, and 2.91 and freestream unit Reynolds numbers of $1.00 - 6.85 \times 10^5$/inch. The focus was on developing effective trips for wind-tunnel studies, so all the trips were placed within an inch of the leading edge. Sublimation was used to detect transition, which was said to occur when the width of the sublimated region began to increase much more rapidly. Figs. 13 and 14, taken from Fig. 6 in Ref. [55], show typical results for triangular and spherical trips at Mach 2.91 and $Re_k = 5500$. The arrows indicate the start of the transverse contamination used as a measure of transition onset, as determined by cathetometer readings. Note that transition occurs farther upstream for the triangular trips (height 0.0146 in.) than for the spherical trips (height 0.015 in.), indicating that triangular trips are more effective. The trips were placed at least three diameters apart, since measurements showed they thereby acted independently. The trips were designed to generate transition well forward of its natural location, which was believed to make the tripped transition independent of freestream noise.

The basic data for x_T vs. Re_k are plotted in detail, along with the natural transition location, and could be reanalyzed, although data for the critical roughness height is not available. To give the flavor of the data, the measurements at the highest M_e and largest x_k are shown in Fig. 15. The data are for a flat plate at $M_e = 2.91$ with trips at $x = 1.00$ in., and the figure was redrawn from Fig. 5r in Ref. [55]. The spherical trips become effective at $Re_k \simeq 8000$, while the triangular trips become effective at $Re_k \simeq 6000$. The unit Reynolds number in the tunnel can be inferred from the value for Re_k and

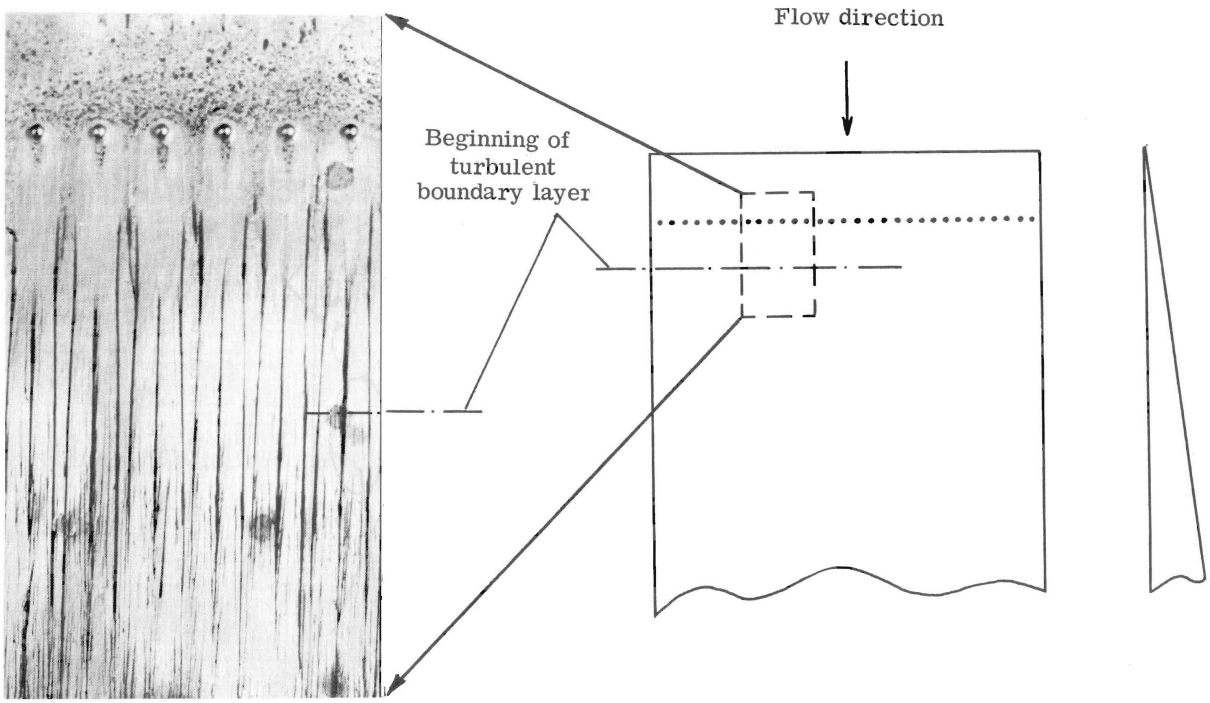

Figure 11: Oilflow Image of Downstream Influence of Spherical Roughness Elements

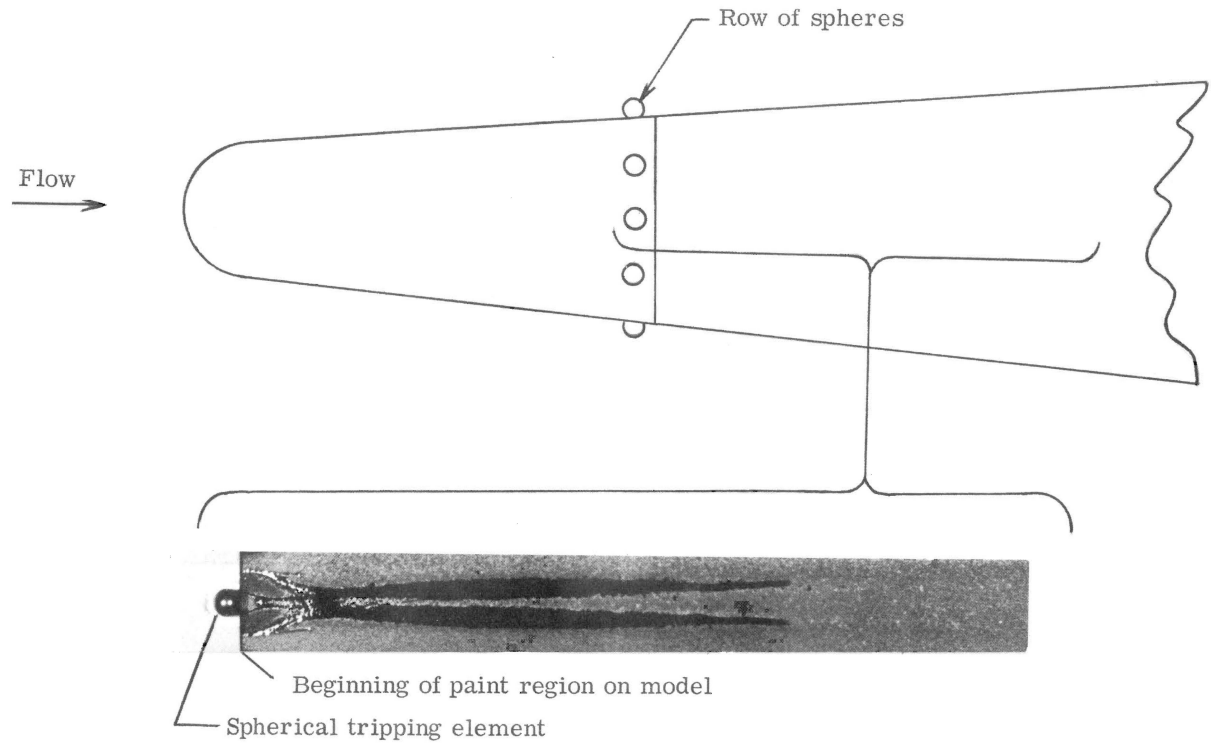

Figure 12: Phase-Change Paint Image of Downstream Influence of Spherical Roughness Elements

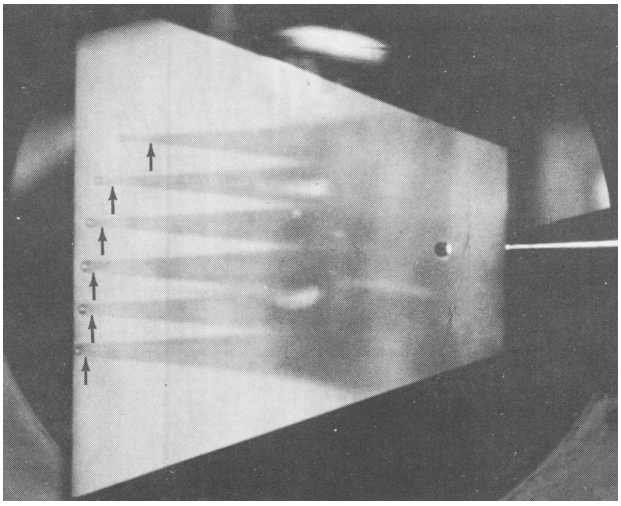

Figure 13: Triangular Trips Visualized Using Fluorene Sublimation

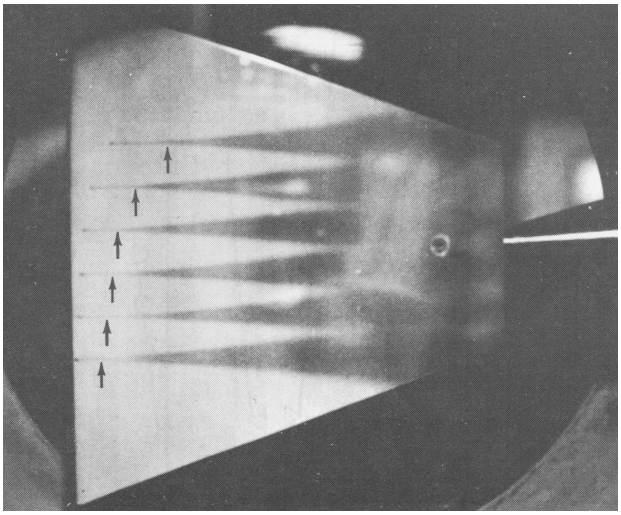

Figure 14: Spherical Trips Visualized Using Fluorene Sublimation

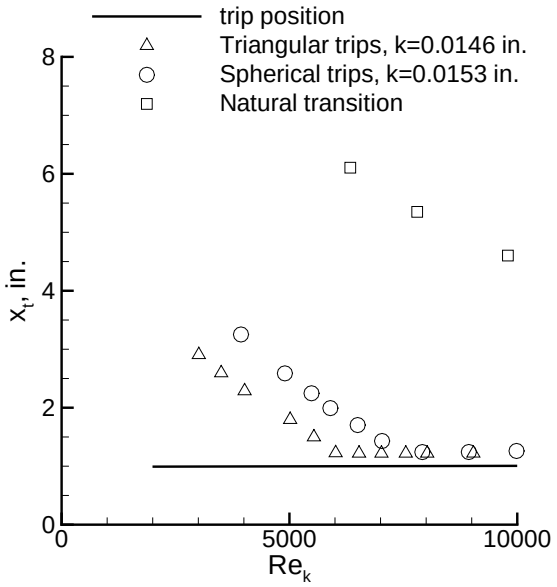

Figure 15: Effect of Trip Reynolds Number on Transition Location

the values for k that are given in the legend. Natural transition moves forward with increasing unit Reynolds number, as would be expected. Although both types of trips move transition far forward of the smooth-wall location, the effect of the triangular trips is clearly larger than that of spherical trips with the same height.

Fig. 16 shows the data for effective tripping conditions, plotted versus the nondimensional trip location. The data are from a flat plate with trips at $x = 0.08 - 1.00$ in., and the figure was redrawn from Fig. 7 in Ref. [55]. The value of Re_k for effective trips ranged from about 1600 to 7300, depending on the downstream location of the trip, x_k, and $M_e = M$, as well as on the type of trip used. Trips are more easily effective when placed farther upstream or operated at lower Mach number. The triangular trips are effective at Reynolds numbers that are roughly 20-40% lower, depending on conditions. When the Mach number is doubled from 1.6 to 2.9, the trips become half as effective, even though the edge Mach number is still not hypersonic. Although the Re_k parameter is useful, it does not come close to correlating all the data.

The need for tripping a hypersonic boundary layer without introducing excessive drag or excessive streamwise vorticity was recently emphasized as part of the development of the X-43A scramjet demonstrator. Berry et al. studied various types of

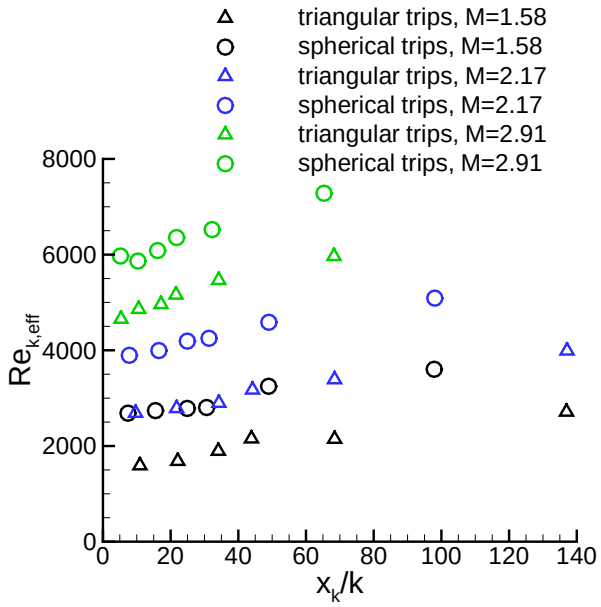

Figure 16: Effect of Station-to-Trip Height on Effective Trip Reynolds Number

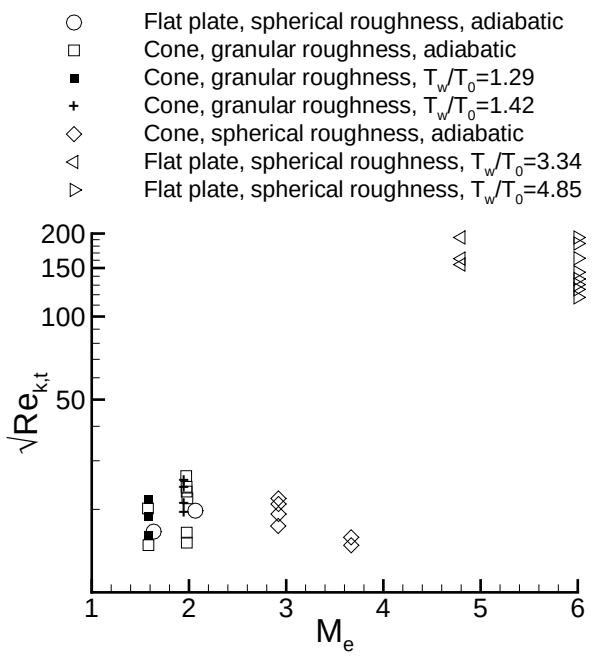

Figure 17: Effect of Mach Number on 'Critical' Roughness Reynolds Number

trips, ending up with a particular swept-ramp vortex generator [56].

Effect of Mach Number on Roughness Effects

The effect of Mach number on roughness effects is dramatic, at high supersonic Mach numbers. Fig. 17, redrawn from Fig. 8 in Ref. [57], is the most striking example. The square root of the *'critical'* roughness Reynolds number is plotted against the edge Mach number. The wall temperature condition is shown in the legend. Braslow points out that $\sqrt{Re_k}$ is proportional to the roughness height, when the roughness is within the linear region of the boundary layer; he also plots two figures which show that the values of $\sqrt{Re_k}$ required to induce transition vary within a band from about 15-45, up to about Mach 4. Between the data at Mach 3.7 and the data at Mach 4.8 and 6, $\sqrt{Re_k}$ increases by a factor of more than 4, so that Re_k increases by an order of magnitude. This is the well known insensitivity of hypersonic flows to being tripped by roughness elements; at least, the effect is well known to the dwindling set of persons familiar with experimental data for hypersonic transition. The plot is striking, but the result is made less clearcut by the measurements in different facilities using different geometries. Braslow reports that the data were taken from the present Refs. [11, 58] and [54]; this and other data should be reanalyzed with modern methods to seek consistent patterns. Unfortunately, Braslow is not clear about his definition of *'critical'* roughness, so without a reanalysis it's difficult to make conclusive statements from his work. However, the reports from which the data were drawn appear to define *'critical'* in substantially different ways.

The data from Holloway and Sterrett which are plotted in Fig. 17 were obtained at a freestream Mach number of 6 on a flat plate in the 20-inch tunnel at NASA Langley [54]. The Mach 4.8 data was obtained by placing the plate at angle of attack; both datasets from Fig. 17 are reproduced with more detail in Fig. 10 of Ref. [54]. Small spheres were spaced spanwise along a line near the leading edge. Holloway and Sterrett define the *'critical'* roughness to be the same as the *'effective'* roughness shown in Fig. 1, so the same is probably true in Fig. 17. Holloway and Sterrett also show $\sqrt{Re_k}$ for effective roughness increasing from about 120 to 200 as the freestream unit Reynolds number increases from 1 to 8 million per foot, for a sharp flat plate at Mach 6, with roughness placed at 2 or 2.87 inches from the leading edge [54, Fig. 11]. Thus, Re_k for effective trips is *not* constant, even for a flat plate of the same geometry at the same Mach number in the same tunnel.

The data from Braslow et al. which are plotted

in Fig. 17 were obtained at freestream Mach numbers of 1.61 and 2.01 in the 4-ft. supersonic tunnel at Langley [58]. A sharp flat plate and a sharp 10-deg. half-angle cone were used. Transition onset was detected via the onset of turbulent bursts as measured with a hot wire near the trailing edge. The roughness was applied in a strip of carborundum grit placed near the leading edge. Braslow et al. define the *'critical'* roughness Reynolds number using the conditions at which the turbulent bursts first appear, a definition closer to the present *'critical'* than to the present *'effective'*; Braslow's work was carried out before such distinctions were later drawn. The mean and maximum roughness height was also measured, for various types of standard carborundum grit. Fig. 9 in Ref. [58] plots $\sqrt{Re_k}$ vs. x_k for cooled and uncooled flat plates and cones, showing values ranging from about 16-24. These data appear to be the same that were later replotted in Fig. 17.

Fig. 18, redrawn from Fig. 6a in Ref. [59], shows a more comprehensive plot of Mach number effects on *effective* roughness. The vertical axis is Re_k for *'effective'* roughness, adjusted using Van Driest's correlation to provide an equivalent value for adiabatic walls. The horizontal axis is the Reynolds number based on edge conditions and the distance from the leading edge to the roughness element. Several datasets are shown; for each, the edge Mach number is given, along with a subscript, with M_P denoting flat plate data and M_C denoting cone data. Three datasets from Van Driest are shown as various types of lines, three datasets from Hicks are shown as various lines with square symbols at the data points, and two datasets from Morrisette are shown as filled and unfilled circles. The results again show an order-of-magnitude increase in Re_k with M_e, although the increase appears much more continuous than in Fig. 17, probably because the dataset is more complete. Note also that Re_k is not constant, even for a given M_e, but depends on $Re_{x,k}$. Although these data and others should be reanalyzed with consistent modern methods, at present these are the two best figures showing the dramatic effect of edge Mach number on roughness effects.

Although the data generated by Hicks was unpublished at the time of Morrisette's paper, it appears that most of the same data was later reported in Ref. [55]. Some of the data is apparently also presented as part of Refs. [60] and [61]. Ref. [62], also by Morrisette et al., appeared after Ref. [59], and contains further information. Fig. 3 in Ref. [62] appears to contain a subset of the data shown here in Fig. 18, along with two more points on the flat

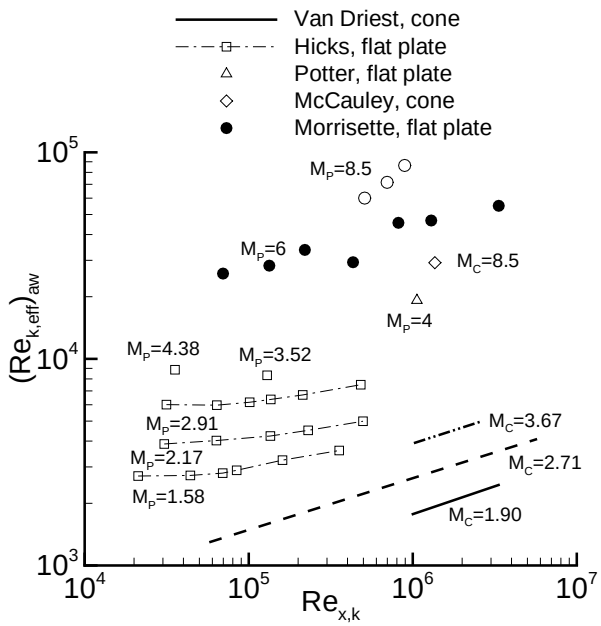

Figure 18: Variation of Effective Roughness Reynolds Number with Roughness Position Reynolds Number and Edge Mach Number

plate at Mach 8 and lower values of $Re_{x,k}$, these two additional points falling on top of the Mach 6 data.

Even with 'effective' trips, transition still occurs some distance downstream of the trip location. With increasing Mach number, transition occurs farther downstream of 'effective' trips. The magnitude of this effect is shown in Fig. 19, redrawn from Fig. 3 in Ref. [59]. The horizontal axis is the edge Mach number for measurements on sharp cones, flat plates, and hollow cylinders. The vertical axis is the Reynolds number based on edge conditions and the location of transition for effective roughness, $Re_{t,eff}$, minus the Reynolds number based on edge conditions and the streamwise location of the roughness elements Re_{x_k}. It is therefore a Reynolds number based on the distance from the trip to the transition location. This Reynolds number increases markedly with Mach number, and is much larger for cones than for flat plates and hollow cylinders. This and other data should be reanalyzed to examine this phenomena further. It may well be associated with the reduced instability of high Mach number shear layers.

It should be noted that in Fig. 19, Klebanoff et al. 1965 is apparently Ref. [16], Van Driest and Blumer is from Ref. [14] and an unavailable North American Aviation report [63] (for which the data

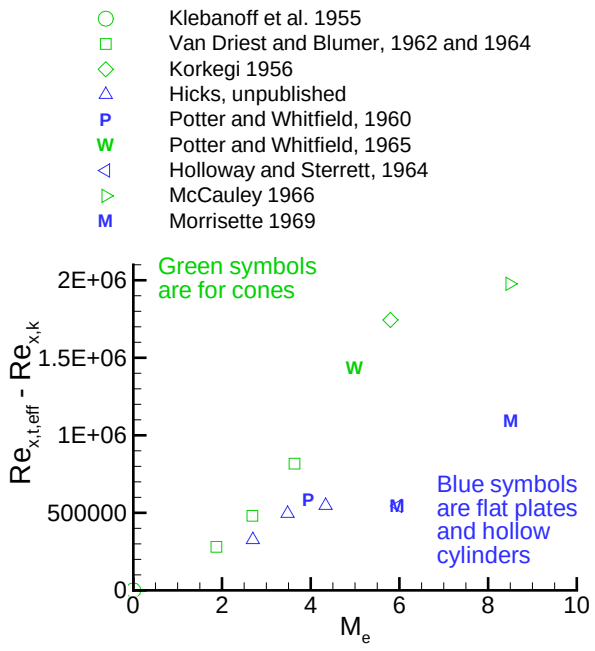

Figure 19: Variation with Mach Number of Reynolds Number Based on Distance from Trip to Transition

may available elsewhere), Korkegi 1956 is from Ref. [64], where this data is actually from sidewall contamination rather than a roughness element, Potter and Whitfield 1960 is from Ref. [65], Potter and Whitfield 1965 is from Ref. [66], Holloway and Sterrett is from Ref. [54], McCauley 1966 is from Ref. [67] (see also Ref. [68]), and the Morrisette 1969 data was generated for Ref. [59].

Effects of Wall Temperature on Roughness Effects

Morrisette et al. review data and correlations for the effect of wall temperature on roughness-induced transition [59]. Their sole non-adiabatic source is unpublished data by A.M. Cary, Jr., obtained on a flat plate at Mach 6, at NASA Langley. They compare a power-law correlation due to Potter and Whitfield to the following correlation due to Van Driest, citing an unavailable report by Van Driest [63]:

$$\frac{Re_{k,eff}}{Re_{k,eff,aw}} = 1 - 0.81\left(\frac{T_{aw}}{T_0} - \frac{T_w}{T_0}\right),$$

where T_{aw} is the adiabatic-wall temperature, T_w is the wall temperature, and T_0 is the stagnation temperature. They find good agreement of Cary's single data point with Van Driest's correlation. Potter and Whitfield's power law overpredicts the wall temperature effect by nearly an order of magnitude.

Wall temperature can have a dramatic effect on roughness effects, since it changes the boundary-layer thickness, as well as other flow properties [69]. Furthermore, the wall-to-total-temperature ratio in wind tunnels often varies dramatically from that expected in flight. Although this issue was studied with some care for the Space Shuttle (e.g., Ref. [70]), it is examined all too rarely. In addition, for most of the data, the wall-temperature ratio is varied by changing the total temperature in the tunnel, which also varies the noise radiated from the nozzle wall. If only the model temperature is varied, then the data are obtained at the same freestream conditions including noise level, but these experiments are complex and difficult and seldom carried out.

Common Approaches for Correlating Roughness Effects on Transition

In the absence of a true theory, many correlations have been developed over the years. Probably the best known is the Re_k approach, popularized recently by Dan Reda of NASA Ames [29, 9]. Arnal et al. reviews four methods in section 5.2 of Ref. [71]; this list is of course incomplete. As a beginning, the following subsections list various approaches which have been popular in various groups over the years.

In the absence of a physics-based theory for the configuration of interest, the present author suggests testing several of these common correlations for experimental data on configurations near those of interest, using roughness types and flow conditions near those of interest, and identifying the correlation which appears to work best. The scatter in the various correlations can be used to estimate the uncertainty in predicting flight. Any such correlation is only as good as the data used to develop it, and although extrapolation is often necessary, it remains risky and uncertain.

Van Driest and Blumer

Ref. [72] correlates roughness-induced transition on cones and hemispheres with $Re_{\delta^\star}/(1+0.5(\gamma-1)M_e^2)$ vs. $(k/\delta^\star)/(1+700(k/D))$, as described above (see also Ref. [14]). It is not certain how well this correlation would extend to other test conditions and other geometries. Ref. [72] follows the all-too-common path of adding additional terms each time a new data set is compared, which makes it unclear if any of these correlations really have any general applicability. Unfortunately, it is laborious and expensive to compare any or all of them to a wide variety of data.

Potter and Whitfield

Potter and Whitfield developed a correlation for the effect of roughness on transition on blunt cones, which has often been used (especially at AEDC) by later researchers [73]. The correlation plots $(x_t/x_{t0})^{1/2} - (Re'_k/\epsilon)(x_k/x_{t0})^{1/2}$ vs. a disturbance parameter Re'_k/ϵ, where ϵ is the value of Re'_k at the location where $x_t = x_k$, x_{t0} is the position of transition on the smooth body, Re'_k is a scaled version of the usual Re_k, and the many other symbols are defined in the reference. This correlation is fairly complex; it has the advantage of estimating how transition moves from the smooth-body location as the roughness is increased, but has the disadvantage of requiring prior knowledge of the smooth-body transition location. Potter et al. show good agreement with many data points from 7 different papers, although many are at low speeds, most are from small-bluntness cones and flat plates. This approach has been used widely over the years and should at least be investigated.

Roughness Reynolds Number Re_k

The roughness Reynolds number $Re_k = \rho_k U_k k/\mu_k$ is probably the single most well supported and well accepted correlation for the effects of roughness on transition. Here, ρ_k, U_k, and μ_k are the density, velocity, and viscosity that are computed in the undisturbed laminar boundary layer at the roughness height k. This correlation has a long heritage in the low-speed arena; the early use at higher speeds was nicely reviewed by Braslow in 1958 [53], who plots several datasets to show that for $M_e \simeq 0 - 2$, a value of $Re_k \simeq 500$ gives a good correlation that fits the effective roughness height within a factor of 2 or so.

Braslow substantiates his claim with three figures. The first, redrawn from Fig. 2 in Ref. [53] as Fig. 20, plots $\sqrt{Re_k}$ for three different flow configurations. In each case, transition is detected via the onset of turbulent bursts measured with a hot wire towards the rear of the model. Thus, this value of Re_k approximates the *'critical'* definition used here. For granular roughness, applied in tripping strips at the location shown on the horizontal axis, $\sqrt{Re_k}$ varies from about 16-27 for a wide range of conditions through low supersonic, as shown in the legend. Braslow argues that the $\sqrt{Re_k}$ is nearly proportional to k, making scatter in $\sqrt{Re_k}$ a good estimator for scatter expected in k.

The second, redrawn from Fig. 3 in Ref. [53] as Fig. 21, plots $\sqrt{Re_k}$ for three different roughness geometries, where d is the particle width or diameter.

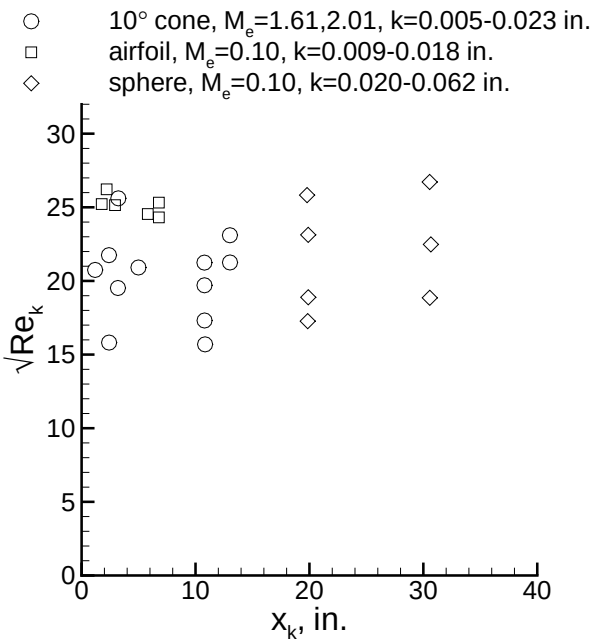

Figure 20: Roughness Reynolds Number for Various Configurations

The circles represent spherical roughness elements, the squares represent granular particles, and the diamonds represent craters with a raised rim around the circumference. For the craters, the overall diameter was used, and the height of the raised rim was used for k. In Figs. 20 and 21, Braslow states that k varies over a factor 12, x_k over a factor 30, d/k over a factor 30, and $M_e = 0 - 2$, yet $\sqrt{Re_k}$ varies only from 15-30, allowing estimation of *'the magnitude of a three-dimensional roughness necessary to cause transition'* to within a factor of 2. This good correlation is expected whenever *'the roughness is well submerged in the boundary layer'*, and is not expected or observed when $k \geq \delta$, based in part on experimental data, and in part on the assumptions made in the dimensional analysis that developed the Re_k parameter.

Braslow makes two good points here, although his definition of 'necessary to cause transition' is vague, perhaps approximating the present 'critical' value, and his datasets are far from comprehensive. Braslow appears to be working from an assumption that the shift in transition location from the smooth-wall value to the roughness position occurs very rapidly (see, e.g., Ref. [74, p. 9]). Although this assumption may be valid in many cases for 3D roughness at low speed, it is not valid in general. In addition, Braslow does not provide data sufficient

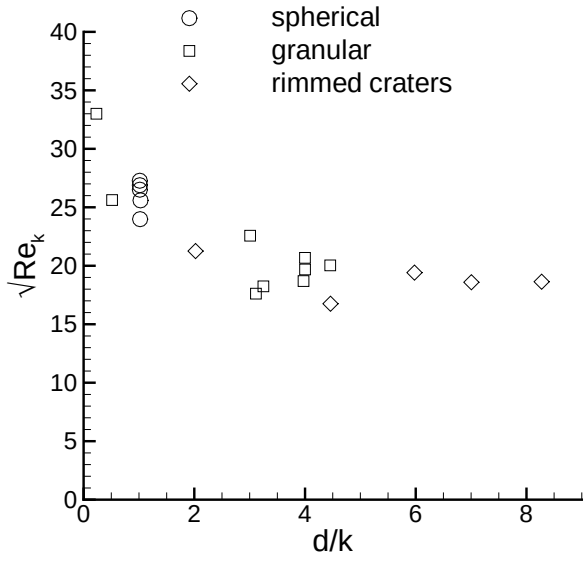

Figure 21: Roughness Reynolds Number for Various Roughness Geometries

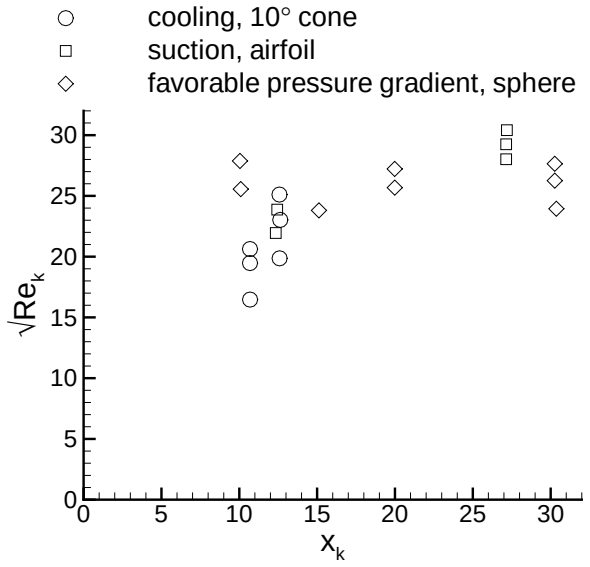

Figure 22: Roughness Reynolds Number Unaffected by Stability Modifiers

to permit reanalysis, although his source references may.

Braslow's third summary figure, redrawn from Fig. 6 in Ref. [53], is shown in Fig. 22. The cone data was obtained for $k = 0.010 - 0.019$ in., at $M_e = 1.61$ or 2.01, with a granular roughness strip. The airfoil data was obtained for $k = 0.004 - 0.012$ in., at $M_e = 0.10$, with cylindrical roughness elements. The sphere data was obtained for $k = 0.015 - 0.062$ in., at $M_e = 0.10$, with spherical roughness elements. In each case, factors that would affect the instabilities leading to smooth-wall transition have little or no effect on roughness-induced transition. The roughness height correlates to within a factor of about 2, since $\sqrt{Re_k}$ varies from 16 to 30. The result is interesting, although the statement cannot be made in general (see, for example, Ref. [23]).

Holloway and Morrisette [74] measured transition in the 20-inch Mach-6 tunnel at Langley using blunt flat plates at zero angle of attack. The spherical roughness elements were placed in a spanwise row behind the leading edge, at the x_k location shown in the legend of Fig. 23. The onset of transition was measured using heat rates inferred from thermocouples. Leading edge A had a 0.188-in. nose radius, and leading edge B a 0.062-in. radius. Detailed drawings of the leading edges are shown in the paper, along with the basic heat-transfer measurements, so reanalysis should be straightforward. Holloway and Morrisette could not reach sufficient Reynolds number to obtain natural transition on the blunt plates, so the natural transition value is not available for correlation. They defined an 'effective' roughness as one for which transition moved to within 0.10 feet of the tripping element. Fig. 23 compares the data to sharp-plate data from Ref. [54]; the figure was redrawn from Figs. 7a and 7b in Ref. [74]. The datasets with $M_e = 3.16$ were obtained on the blunt plate, assuming a normal-shock pressure loss.

The open symbols are for roughnesses just less than effective, while the closed or thick-lined symbols are for roughness elements just greater than effective. Four separate conditions are thus shown, with the green symbols showing Re_k, referred to the left-hand axis, and the blue symbols showing k/δ, referred to the right-hand axis. The boundary-layer thickness δ was computed from theory. Although Re_k gives a good nearly-constant correlation for the blunt-plate data, it rises by a factor 3 with increasing unit Reynolds number, for the sharp-plate data. This is consistent with Braslow's earlier hypothesis that Re_k correlates well for low M_e, where $k < \delta$. However, the blue symbols show that $k > \delta$ for all of the data, as well as that k/δ is not constant for any of the data. Thus Braslow's hypothesis is not tested here; the blunt-plate data simply add an additional point, that Re_k can sometimes correlate well even when $k > \delta$. This clean and well documented

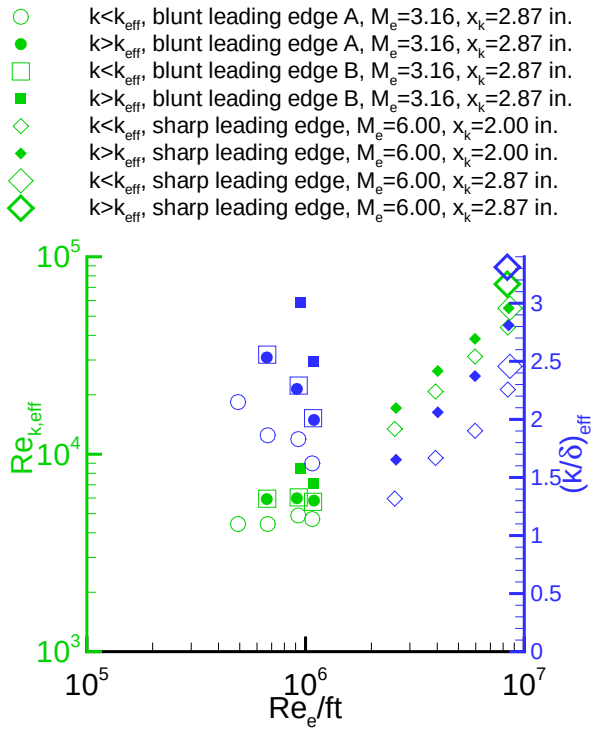

Figure 23: Variation of Effective Roughness Parameters with Unit Reynolds Number at $M_\infty = 6$

dataset clearly shows that Re_k is not a universally valid correlation, even for particular conditions like flat plates at a particular Mach number. The data should be reanalyzed with modern methods.

In recent years, this correlation has been advocated by Reda [9]. Reda's review should be consulted for additional examples of this approach. In Ref. [9], Reda points out that several other common correlations for transition on attachment lines, lifting reentry vehicles, and blunt bodies can be more simply recast in terms of Re_k. Reda had to make a number of simplifying assumptions in recasting the other correlations, due to limited resources. Here again, it would be interesting to see a full reanalysis of these cases, comparing the results to several correlations, if resources become available for recomputing these flows.

PANT Correlation for Blunt Nosetips

Wool [75] is the basic reference that is available in the open literature. In addition, Ref. [28] was approved for public release in the last few years. Wool recommends the 'PANT transition onset criterion' of

$$Re^\star_\theta \left(\frac{k}{\psi^\star \theta^\star}\right)^{0.7} = 255,$$

where

$$\psi^\star = 0.1B' + (1 + 0.25B')\frac{\rho_e}{\rho_w},$$

and values with the superscript $\star$ are taken at the sonic conditions [28, Fig. 10]. Here, $B' = \dot{m}/\rho_e u_e C_H$, a nondimensional ablation parameter, where C_H is the Stanton number, $\dot{m}$ is the surface ablation mass flux, ρ_e is the density at the boundary-layer edge, ρ_w is the density at the wall, and k is here the peak-to-valley roughness height. Wool's Fig. 10 compares the correlation to 11 datasets on hemispherical noses with radii varying from 0.75 to 5.0 inches, roughness heights varying from 0.0006 to 0.010 inches, and stagnation temperatures varying from $1000 - 1350°R$.

Swigart presented a modified PANT correlation for $Re_{\delta^\star_T}/(1 + 0.5(\gamma - 1)M^2_{e,T})$ vs. $(k/\delta^\star_T)/(1 + 350(k/R_N))$. Here, $\delta^\star$ is displacement thickness, R_N is nose radius, and $M_{e,T}$ is the edge Mach number at the transition location. Swigart compares 5 datasets with reasonable agreement [76]. See also the discussion in the previous section describing Previous Reviews [30, 29].

Boudreau Correlation for Trips on Sphere-Cone Nosetips

Boudreau developed a method for tripping the boundary layer on the frustum of hypersonic sphere-cones using relatively small roughness distributed over the nosetip [77]. The correlation is supported with seven datasets at Mach 6-13 in Tunnels B and F at AEDC, and also with PANT data. Boudreau found that distributed roughness allowed tripping with much smaller roughness heights than was necessary using rows of isolated roughness elements. He correlated transition immediately behind the trip location with

$$\lambda^\star_{M,\text{critical}} \simeq 800,$$

where

$$\lambda^\star_M = X\frac{k}{r_n}\left(\frac{P_E}{P'_0}\right)^{0.9}(Re_{\infty,r_n})^{1.2},$$

$$X = Re^\star_{e,\theta}\left[\frac{T^\star_e}{T_w}\frac{r_n}{\theta^\star}\right]^{0.7}(Re_{\infty,r_n})^{-0.85},$$

the superscript $\star$ indicates evaluation at sonic-point conditions, r_n is the nose radius, P_E is the pressure at the end of the roughness area, at $s/r_n = 5$, near the end of the overexpansion from the nose-frustum

junction, s is arclength from the stagnation point, P_0' is the freestream pitot pressure, and Re_{∞,r_n} is a Reynolds number based on freestream conditions and nose radius. This correlation and the preliminary suggestion of Stetson [78] are the only available methods for estimating transition on a cone frustum due to roughness on the nosetip (see Ref. [5]).

Shuttle Roughness Criteria

Transition on lifting reentry vehicles with low ballistic coefficients has been studied by NASA for the Space Shuttle, X-33, X-34, and X-38 programs. For the Shuttle, transition is thought to be dominated by roughness effects [79], and the other three vehicles were also often expected to be roughness-dominated, although they never flew. The Shuttle has been studied by a variety of investigators over many years, but since the middle 1970's the majority of the work has been carried out by Bertin et al. and Berry et al.

Berry et al. reviewed the correlation for roughness-induced transition that was developed at NASA Langley [80]. Berry et al. plot the roughness height divided by the boundary-layer thickness, k/δ, against Re_θ/M_e, where Re_θ is based on momentum thickness and edge conditions. They correlate effective isolated-roughness data from the Mach-6 tunnel at Langley using $(Re_\theta/M_e)(k/\delta) = 70$, for Shuttle, X-33, and X-38, using an inviscid computation coupled with an integral-method boundary-layer code. The computational method that is used to compute the correlating parameters is shown to be critical to accuracy, since a change in method from the BLIMP to LATCH codes affects the correlating value of Re_θ/M_e by a factor of two (their figure 1). Note that BLIMP is a finite-element boundary-layer code, and LATCH is an integral-method boundary-layer code. A similar correlation of incipient-roughness data for Shuttle is also shown.

The precise definition of δ is difficult to determine, since it is found from the correlation contained in the integral-method boundary-layer code. However, Berry et al. also show good correlation for the Shuttle with $(Re_\theta/M_e)(k/\theta) = C$, where $C = 200$ for critical or incipient roughness effects, and $C = 310$ for effective roughness. Although the reduction of data for three separate models to one correlation is fairly impressive, all three datasets were obtained in the same wind tunnel at the same Mach number and wall-temperature ratio, for similar geometries, and critical or incipient roughness effects are not compared for different geometries, so the generality of this correlation remains to be determined.

Bertin et al. performed a series of experiments in AEDC Tunnel B over many years, as most recently reported in Ref. [81]. For these discrete roughness measurements carried out ca. 1995, Bertin et al. report that *'For the present tests, $Re_\theta, Re_\theta/M_e$, and Re_k were found to be the most useful correlation parameters. Correlations using roughness height relative to parameters associated with the boundary-layer thickness, e.g., $k/\delta, k/\delta^\star$, and k/θ, failed to provide consistent results.'* To determine if a correlation is really general and independent of tunnel noise, data from all the tunnels should be compared using several different correlations to see how well they work. Such a study remains to be performed for the Shuttle.

Spreading Angle of Turbulent Wedges from Roughness Elements

Fischer reviewed a wide variety of data for the spreading angle of the turbulent wedges that convect aft from roughness elements [82]. Fischer shows that the spreading angle decreases with increasing Mach number. However, Ref. [11] gives a spreading angle that *increases* from 5 to 7 deg. as the edge Mach number increases from 1.9 to 3.67, a trend opposite to that shown by Fischer. Although Fischer's result is often quoted and seems physically reasonable, the problem remains to be studied with care. For example, the effect of tunnel noise has never been evaluated.

Designing Surface Roughness Large Enough to Trip Transition

Wind tunnels at all speed ranges are rarely able to simulate the very high Reynolds number of full-scale vehicles. This is particularly true for hypersonic conditions, where achieving high Reynolds numbers is more difficult in wind tunnels. Since one of the primary effects of Reynolds number is the location of transition, roughness has often been used to trip the boundary layer to turbulence further upstream, in an attempt to simulate the location of transition in flight. The hypersonic case is more difficult to trip, since the hypersonic boundary layer is insensitive to roughness. The location of transition and the drag of the trips used to affect it are then a part of the drag budget that is used to estimate efficiency in flight. The accuracy of this drag budget is often critical [83].

An issue related to tripping is the properties of the tripped boundary layer relative to those of a

naturally turbulent boundary layer, or one tripped using a different approach. Trips add trip drag and streamwise vorticity, change the boundary layer thickness, and change the heat transfer and skin friction. Daugherty and Hicks measured the skin friction on a flat plate at Mach 2.17, using a floating element [84]. They found that skin friction depended only weakly on the height of the trips, for k/δ ranging from 1.1 to 7.5. Morrisette et al. also review information regarding the drag of trips [59]. They plot the drag coefficient for the trips based on conditions at the boundary layer edge, and find that spheres have the highest drag. Sterrett et al. show that a tripped hypersonic boundary layer can have the same heat transfer as a turbulent boundary layer that develops naturally [60, Fig. 2]. They reiterate that the roughness Reynolds number required to trip a flow rises dramatically with M_e. They also. discuss the drag of the roughness elements.

The distortion of the turbulent boundary layer is also an issue for some applications. Sterrett et al. show in an oilflow image that the vortex wakes of large elements can slowly disappear as they travel down a flat plate, and then reappear after passing through a compression corner (Ref. [60]; see also Fig. 2). Peterson measured the distortion of the boundary layer profiles on a flat plate at Mach 3 and 4, using a pitot tube [85]. The trips were placed within 1 cm of the leading edge, and the profiles were measured 21.6 cm from the leading edge. Natural smooth-wall transition occurred at about 5 cm from the leading edge, so the trips didn't generate transition at the measurement location, they just influenced a boundary layer which was already turbulent. The nondimensional profiles depended only weakly on the trip, but the boundary layer thicknesses increased by a factor of up to 2 as the trip height increased to 0.5 mm. The measurements were tabulated and plotted in detail.

Braslow et al. discusses tripping issues, mostly with respect to the development of supersonic transports [61], but pointing out that hypersonic edge Mach numbers require large trips that tend to generate a lot of trip drag and a highly disturbed boundary layer. For edge Mach numbers of about 2 or less, Braslow et al. argue that $Re_k \simeq 600$ is both a *critical* and *effective* criteria, and should be used for trip designs, as long as $Re_{x,k} > 2 \times 10^5$. However, for $M_e > 2$, the required trip height rises dramatically, and an *effective*-height trip becomes much larger than a *critical*-height trip.

Designing Surface Roughness Small Enough to Have No Effect

How smooth does a surface have to be so that roughness does not cause transition earlier than on a yet smoother surface? In other words, what is the specification on roughness that makes a surface smooth enough to be free of roughness effects on transition? This question often arises in design.

An excellent review by Smith and Clutter found that $Re_k \simeq 25$ gave a good estimate for the smallest height of roughness that is capable of affecting transition at low speeds [15]. Beckwith used $Re_k \simeq 12$ to design laminar-flow supersonic nozzles sufficiently smooth so that the roughness does not dominate transition, with k being the largest roughness height anywhere on the surface [86]. For these quiet-nozzle designs, the thin boundary layer makes the transonic throat the most sensitive area, and this $Re_k \simeq 12$ criteria has proved useful, although it includes much uncertainty.

However, Radeztsky et al. found that roughness with $Re_k < 1$ was still sufficient to generate streamwise vorticity that amplified through the stationary crossflow instability and had a significant effect on transition for low-speed swept wings [23]. On the other hand, for hypersonic edge Mach numbers on symmetric vehicles such as sharp cones at zero angle of attack, very large roughness elements with $Re_k > 10^4$ are required to trip the flow (Fig. 18).

Thus, it appears there is no general answer to this question, at least at present. In general, roughness with $Re_k < 10 - 25$ is unlikely to affect transition, unless there is a mechanism for amplifying weak streamwise vorticity so that it dominates transition – such mechanisms would include the crossflow [3], Görtler [1], and transient-growth instabilities [48]. In many cases, this criteria may be very difficult and expensive to satisfy, and it may be much more stringent that is necessary, for example at high edge Mach numbers. The flowfield of interest then needs to be studied in more detail to provide more refined criteria.

Additional Comments Regarding Distributed Roughness

The effects of distributed roughness are complex, difficult to measure, and poorly understood. Although the topic is therefore often avoided, it is always a part of the actual development of ground and flight experiments. Particular isolated roughness elements are inherently easier to study, since the source of the

disturbances is localized, and can be controlled and measured in detail. For distributed roughness, it is often the largest isolated local flaw that dominates the effect of roughness on transition. However, it is often very difficult to determine the largest local flaw except by extensive iteration, measuring transition and how it changes when the roughness is modified (see, e.g., Ref. [87]). Modern instrumentation does allow the mapping of microroughness elements in a surface [88], *if* the surface is sufficiently accessible. However, it is difficult to imagine actually measuring the largest microroughness by scanning a microinterferometer over a large contoured surface; the process would be too difficult and expensive. Instead, the largest roughness elements are usually picked out by visual inspection, which only works well when the RMS roughness is much smaller than the largest flaws.

It is difficult even to estimate critical and effective values for distributed roughness, since the roughness height relative to boundary-layer thickness varies as the boundary layer grows downstream, and the portions of the roughness that contribute to transition are almost never known. It is usually best to begin by determining the worst-case values of a correlating roughness parameter, examining the whole surface [89, pp. 28-30]. However, unless there is a solid understanding of how the roughness contributes to transition, this can only be taken as a crude first approximation.

Real vehicles often develop surface roughness in flight which is not present before launch. This flight-induced roughness may be due to steps and gaps caused by thermal expansion. It may also involve steps, gaps, and distributed roughness induced by ablation, or the impact of dust, water or ice droplets, or insects. In many cases the roughness in flight can be estimated from computations of ablation or thermal expansion, or from experiments under representative conditions in an arcjet. Extensive and painstaking experimental work is at present the only method of addressing these complexities.

Case Studies

There is an immense literature for roughness effects on hypersonic transition for various geometries and conditions. The following subsections highlight a few particular examples.

Measurements with Distributed Roughness

Jones measured heat transfer to 10-deg. half-angle sharp cones in a Mach 5 blowdown tunnel at NASA Langley [90]. The very high freestream unit Reynolds numbers ranged from $20 - 100 \times 10^6$/ft. Four different models were tested, with surface finishes of about 2, 7, 15, and 65 microinches. All had 2-inch base diameters. The characteristics of the roughness were measured and discussed in some detail. In the one case analyzed in some detail, transition occurred at $Re_k \simeq 400$. These data may be worthy of reanalysis. This value of Re_k seems fairly low for an edge Mach number of roughly 4, perhaps because of the distributed roughness. This data is included here due in part to the rarity of controlled measurements with distributed roughness.

Space Shuttle Orbiter

Goodrich et al. examined the flight data for the Shuttle, and compared it to ground tests, using correlations (see Ref. [91], which is an updated version of Ref. [92] that includes data from the fifth flight). This 1983 review was the first of several; it followed shortly after the first five 'test' flights, before the shuttle was declared 'operational'. Goodrich gives a clear explanation of the logic behind the correlations used to predict transition on the Shuttle. Only centerline data was considered, in large part because the centerline was the only location where the boundary-layer properties could be computed. For centerline locations forward of 40% of the vehicle length, surface roughness appeared to dominate transition, since the flight data correlated well with the wind tunnel data. However, for locations aft of 40%, tunnel noise apparently played a dominant role, for transition in flight occurred much later than in the wind tunnel.

A large amount of data has been published for the Shuttle geometry over many years (see, for example, Ref. [93]). A comprehensive review of roughness effects on Shuttle transition would require a separate paper; thus, the brief discussion provided here can only serve as an introduction. In particular, several of the popular correlations should be compared to a comprehensive set of Shuttle data from both flight and ground test, so that the pros and cons of the various correlations can be identified. However, such a comparison would be an extensive research project in itself, for which no resources are presently available.

X-17 Flight Data

The X-17 program flew 26 hemispherical noses with an 9-inch diameter to roughly 13,000 ft/sec., using a three-stage rocket [94, 8]. The nickel-plated copper noses were polished to various surface finishes, and transition was inferred from heating rates

on thermocouples placed along several rays. Tellep provides a detailed description of the 26th flight, along with a summary of the roughness-effects information from the first 25 flights, including transition data from flights 2, 8, 9, 11, and 22 [94]. Although Ref. [94] is public release, many of the other flight reports are not yet in the public domain. The momentum-thickness Reynolds number is computed at transition onset, but no roughness correlations are provided. For several flights, roughness patches were placed on the highly polished surface along different rays, with thermocouples, to determine roughness effects. Rays of control thermocouples were still always placed along the smooth surface.

Unfortunately, Tellep's analysis is focused on the effect of the average roughness, which was 1/2 microinch RMS for the 26th flight, with two patches roughened to 45 microinches. Table IV in Ref. [94] details 10 pits in the surface that are many times larger than the background roughness, with depths ranging from 15 to 60 microinches, but these pits are not analyzed further. It appears that transition on the nominally smooth portions of these vehicles may well have been tripped by the flow over these pits. It would be useful to reanalyze this data using the usual roughness correlations, to see if the roughness heights or the pits can explain the pattern of transition onset in the six flights described by Tellep.

Attachment Lines on Leading Edges

Several classes of hypersonic vehicles have attachment lines on leading edges with small nose radii, producing thin boundary layers that can be very sensitive to roughness, similar to those on transonic transport planes. These include winged vehicles like the Shuttle and vehicles with delta-wing bodies. Reda showed that Poll's criteria for roughness effects on these attachment lines [95] can be recast in terms of the Re_k criteria [9]. Several papers have been published in this area in the last two decades, for both smooth and rough surfaces, usually using swept cylinders, and a comprehensive review is needed here also.

Summary

The effect of roughness on hypersonic laminar-turbulent transition has been reviewed. Roughness may consist of isolated flaws or trips, such as steps, gaps, or spheres placed on the wall, or of distributed flaws, such as machining marks, sandpaper, or ablation-induced irregularities. As the height of the roughness increases from insignificant to *'critical'*, it begins to affect transition far downstream of the roughness element, moving it forward from the smooth-wall location. As the height increases still further, it reaches the *'effective'* level, where transition occurs a relatively short distance behind the roughness element, and further increases in roughness height do not reduce this distance. Tunnel noise is likely to have a substantial effect on transition for roughness elements larger than 'critical' but smaller than 'effective'.

Roughness generates a wake within the boundary layer, with streamwise vorticity, and roughness of sufficient height generates a bow shock. There seem to be three modes by which the roughness may affect transition. Instabilities may grow in the wake of the roughness element, and may cause transition to turbulence, before the wake dissipates downstream due to viscous effects. The streamwise vorticity that trails the roughness may grow via crossflow, Görtler, or transient-growth mechanisms, leading to transition downstream. Finally, freestream disturbances such as acoustic waves may interact with surface roughness to generate boundary-layer disturbances such as first-mode or second-mode waves, which then amplify and cause transition downstream. The effect of roughness thus depends on the flowfield it is placed within.

The roughness Reynolds number computed using conditions in the undisturbed laminar boundary layer at the roughness height, Re_k, is the most common of the various correlating formulas, and is probably of the most general applicability. The determination of Re_k requires laminar boundary-layer profiles, but with modern computational tools this is relatively simple. For both critical and effective roughness, Re_k increases by two orders of magnitude as the edge Mach number rises from subsonic to hypersonic. This is probably caused by the generally smaller instability of high-Mach-number shear layers. Since the values of Re_k at which roughness affects transition vary widely, depending on conditions, it can only be used as a first approximation.

Recommendations for Future Research

Much research remains to be carried out. Several of the common correlations should be computed for a wide variety of data, using the same modern computational tool, to determine if any of the correlations have any general applicability. Braslow argues that the Re_k criterion should have general applicability

when the roughness height is small compared to the boundary-layer thickness; this interesting hypothesis should be tested.

More fundamentally, it is now becoming feasible to develop roughness-induced transition predictions based on the instabilities of the wake of the roughness element, at least for some conditions. Modern computational tools are making it possible to extend Klebanoff's approach from 2D roughness elements on flat plates at low speed to any kind of isolated roughness element at any speed. A mechanism-based prediction method of this type holds great promise for reducing the uncertainty in extrapolating ground-test data for prediction of flight conditions.

For transition induced in part by the growth of streamwise vorticity from small roughness elements, the receptivity problem for crossflow, Görtler, and transient-growth instabilities needs to be solved; this work is in the very early stages. The study of freestream disturbances interacting with surface roughness to generate instabilities has made great strides for acoustic waves interacting with flat-plate roughness at low speeds. However, much remains to be done for other forms of freestream disturbances, other model geometries, and higher speed ranges.

Recommendations for Vehicle Designers

There is as yet no scientific theory for estimating the effect of roughness on transition. Rather, the effects of roughness on transition must be evaluated using empirical wind-tunnel experiments under conditions that mimic flight as much as possible. Experiments should be carried out on models with varying levels of roughness at varying conditions, and the results from several wind tunnels can then be correlated with one of several algebraic formulas. Several common algebraic correlations are given here; these remain useful, although none have general applicability. The data summarized here should aid in selecting among these correlations, and in evaluating likely values for the correlating parameters. These formulas can then be used to extrapolate the ground-testing results to flight. The risk of surprises will be lower if the instabilities leading to smooth-wall transition can be determined, since the effect of roughness on the smooth-wall instabilities can then be assessed. The resources devoted to estimating transition should depend on the effect on the design of the uncertainty in transition.

There are several sources of uncertainty in this empirical approach: (1) the inability of any single wind tunnel to simultaneously reproduce the Mach number, Reynolds number, wall-temperature ratio, gas chemistry, noise levels, and surface ablation of hypersonic flight, (2) the scatter in any empirical correlation when tested against data from a variety of wind tunnels, (3) the uncertainty in extrapolating a correlation from ground test to flight, and (4) the actual as-heated and as-ablated surface roughness in flight. However, this approach is the best that is presently available. The scatter in the results from various wind tunnels can be used to estimate the uncertainty in the various correlations, and the scatter involved in extrapolating the various correlations to flight can be used to estimate the uncertainty in the flight prediction.

Acknowledgements

Many persons, too numerous to mention, have drawn attention to various data and references. Figure 7 is reprinted by permission of the Instrumentation Society of America, per a 7 Dec. 2006 email from Eugenia Bell, as it was copyrighted by ISA in 1979, with all rights reserved. Dr. Daniel Reda of NASA Ames provided a high-quality scan from a viewgraph he had saved. Dr. Richard Batt from TRW sent the author a pallet of papers on roughness-induced transition when he retired in 1997. Dennis Bushnell from NASA Langley first drew attention to Fig. 17. Prof. Eli Reshotko from Case Western Reserve University drew the author's attention to the 1972 paper by Klebanoff and Tidstrom; his advice and encouragement over the past 17 years is greatly appreciated. Mr. Garland Gouger from the NASA Langley library provided high-quality scans from original paper copies for Figs. 8, 13, and 14. The author has been able to focus his research on hypersonic transition for the last 17 years, thanks to support primarily from AFOSR, Sandia National Laboratories, and NASA. AFOSR has enabled the effort by providing consistent long-term support over some dozen years under three different program managers: Len Sakell, Steve Walker, and John Schmisseur.

REFERENCES

[1] William S. Saric. Görtler vortices. *Annual Review of Fluid Mechanics*, 26:379–409, 1994.

[2] L. M. Mack. Boundary layer linear stability theory. In *Report 709, Special Course on Stability and Transition of Laminar Flow*, pages 1–81. AGARD, March 1984.

[3] W.S. Saric, H.L. Reed, and E.B. White. Stability and transition of three-dimensional boundary layers. *Annual Review of Fluid Mechanics*, 35:413–440, 2003.

[4] D. Arnal and G. Casalis. Laminar-turbulent transition prediction in three-dimensional flows. *Progress in Aerospace Sciences*, 36:173–191, 2000.

[5] Steven P. Schneider. Hypersonic laminar-turbulent transition on circular cones and scramjet forebodies. *Progress in Aerospace Sciences*, 40(1-2):1–50, 2004.

[6] I.E. Beckwith and C.G. Miller III. Aerothermodynamics and transition in high-speed wind tunnels at NASA Langley. *Annual Review of Fluid Mechanics*, 22:419–439, 1990.

[7] Steven P. Schneider. Effects of high-speed tunnel noise on laminar-turbulent transition. *Journal of Spacecraft and Rockets*, 38(3):323–333, May–June 2001.

[8] Steven P. Schneider. Flight data for boundary-layer transition at hypersonic and supersonic speeds. *Journal of Spacecraft and Rockets*, 36(1):8–20, 1999.

[9] Daniel C. Reda. Review and synthesis of roughness-dominated transition correlations for reentry applications. *J. of Spacecraft and Rockets*, 39(2):161–167, March-April 2002.

[10] S.R. Pate. Supersonic boundary-layer transition: effects of roughness and freestream disturbances. *AIAA Journal*, 9(5):797–803, May 1971.

[11] E.R. Van Driest and W.D. McCauley. The effect of controlled three-dimensional roughness on boundary-layer transition at supersonic speeds. *Journal of the Aeronautical Sciences*, 27(4):261–271 plus 303, April 1960.

[12] S.R. Pate and C.J. Schueler. Radiated aerodynamic noise effects on boundary-layer transition in supersonic and hypersonic wind tunnels. *AIAA Journal*, 7(3):450–457, March 1969.

[13] S. R. Pate. Dominance of radiated aerodynamic noise on boundary-layer transition in supersonic/hypersonic wind tunnels. Technical Report AEDC-TR-77-107, Arnold Engineering Development Center, Arnold Air Force Station, Tennessee, March 1978.

[14] E.R. Van Driest and C.B. Blumer. Boundary-layer transition at supersonic speeds – three-dimensional roughness effects (spheres). *J. of the Aerospace Sciences*, 29:909–916, August 1962.

[15] A.M.O. Smith and D. W. Clutter. The smallest height of roughness capable of affecting boundary-layer transition. *Journal of Aerospace Sciences*, 26(4):229–245, April 1959.

[16] P.S. Klebanoff, G.B. Schubauer, and K.D. Tidstrom. Measurements of the effect of two-dimensional and three-dimensional roughness elements on boundary-layer transition. *Journal of the Aeronautical Sciences*, 22:803–804, November 1955.

[17] P.S. Klebanoff, W.G. Cleveland, and K.D. Tidstrom. On the evolution of a turbulent boundary layer induced by a three-dimensional roughness element. *J. Fluid Mechanics*, 237:101–187, 1992.

[18] H. L. Dryden. Transition from laminar to turbulent flow. In C.C. Lin, editor, *Turbulent Flows and Heat Transfer*, pages 3–74. Princeton University Press, Princeton, New Jersey, 1959. Volume V in the series on High Speed Aerodynamics and Heat Transfer.

[19] H. L. Dryden. Review of published data on the effect of roughness on transition from laminar to turbulent flow. *J. Aeronautical Sciences*, 20:477–482, July 1953.

[20] H. L. Dryden. Combined effects of turbulence and roughness on transition. *Zeitschrift für angewandte Mathematik und Physik (ZAMP)*, 9b:249–258, 1958.

[21] Albert E. Von Doenhoff and Albert L. Braslow. The effect of distributed surface roughness on laminar flow. In Gustav Lachmann, editor, *Boundary layer and flow control, volume 2*, pages 657–681. Pergamon Press, New York, 1961.

[22] Itiro Tani. Effect of two-dimensional and isolated roughness on laminar flow. In Gustav

Lachmann, editor, *Boundary layer and flow control, volume 2*, pages 637–656. Pergamon Press, New York, 1961.

[23] R.H. Radeztsky, M.S. Reibert, and W.S. Saric. Effect of isolated micron-sized roughness on transition in swept-wing flows. *AIAA J.*, 37(11):1370–1377, November 1999.

[24] F. Gökhan Ergin and Edward B. White. Unsteady and transitional flows behind roughness elements. *AIAA Journal*, 44(11):2504–2514, November 2006.

[25] Itiro Tani. Boundary-layer transition. *Annual Reviews of Fluid Mechanics*, 1:169–196, 1969.

[26] Albert L. Braslow. Review of the effect of distributed surface roughness on boundary-layer transition. Report 254, AGARD, April 1960.

[27] Neal Tetervin. Transition, minimum critical, minimum transition, and roughness Reynolds numbers, for seven blunt bodies of revolution in flight between Mach numbers of 1.72 and 15.1. Technical Report NOL-TR-62-25, Naval Ordnance Laboratory, August 1962. Citation AD333238 in DTIC.

[28] M.R. Wool. Final summary report, passive nosetip technology (PANT) program. Technical Report TR-75-250, SAMSO, January 1975. Citation AD-A019186 in DTIC.

[29] Daniel C. Reda. Correlation of nosetip boundary-layer transition data measured in ballistics-range experiments. *AIAA Journal*, 19(3):329–339, March 1981.

[30] R. G. Batt and H.H. Legner. A review of roughness-induced nosetip transition. *AIAA Journal*, 21(1):7–22, January 1983.

[31] M.L. Finson. Advanced reentry aeromechanics, interim scientific report, an analysis of nosetip boundary layer transition data. Report PSI-TR-52, Physical Sciences, Inc., August 1976. AFOSR-TR-76-1106.

[32] M.L. Finson, A.N. Pirri, P.E. Nebolsine, G.A. Simons, and P.K.S. Wu. Advanced reentry aeromechanics; final report. Report PSI-TR-115, Physical Sciences, Inc., January 1978. AFOSR-TR-78-0607TR, citation 78N25117 in NASA STI, citation AD-A052744 in DTIC.

[33] William M. Bishop. Transition induced by distributed roughness on blunt bodies in supersonic flow. Paper 77-124, AIAA, January 1977.

[34] William M. Bishop. Transition induced by distributed roughness on blunt bodies in supersonic flow. Technical Report TR-76-146, SAMSO, October 1976. DTIC citation AD-A032009.

[35] John J. Bertin. *Hypersonic Aerothermodynamics*. AIAA, Washington, DC, 1994.

[36] Steven P. Schneider. Laminar-turbulent transition on reentry capsules and planetary probes. *Journal of Spacecraft and Rockets*, 43(6):1153–1173, Nov.-Dec. 2006.

[37] Steven P. Schneider. Transition on blunt bodies with roughness and ablation. Paper 2008-XXXX, AIAA, January 2008. A 35-page manuscript with 8 figures and 96 references. To be submitted to the Aerospace Sciences Meeting.

[38] Edward B. White, Robert S. Downs III, and Hillary C. Emer. Disturbances generated by random and periodic surface roughness: experiments and models. Paper 2006-3526, AIAA, June 2006.

[39] Daniel C. Reda. Comparative transition performance of several nosetip materials at defined by ballistics-range testing. In *Proceedings of the 25th International Instrumentation Symposium held May 7-10, 1979, Anaheim, California*, pages 89–104, May 1979. See also the journal version in ISA Transactions, vol. 19, no. 1, Jan. 1980.

[40] James L. Hunt and Robert A. Jones. Effects of several ramp-fairing, umbilical, and pad configurations on aerodynamics heating to Apollo command module at Mach 8. Technical Memorandum NASA-TM-X-1640, NASA, September 1968.

[41] Max E. Wilkins and John F. Darsow. Finishing and inspection of model surfaces for boundary-layer-transition tests. Memorandum NASA-MEMO-1-19-59A, NASA, February 1959. NASA STI citation 19980232015.

[42] P. Klebanoff and K. Tidstrom. Two-dimensional roughness element induces boundary-layer transition. *Physics of Fluids*, 15(7):1173–1188, 1972.

[43] H. W. Liepmann and Gertrude H. Fila. Investigations of effects of surface temperature and single roughness elements on boundary-layer transition. Report 890, NACA, 1947.

[44] Mark V. Morkovin. On the many faces of transition. In C. Sinclair Wells, editor, *Viscous Drag Reduction*, pages 1–31. Plenum Press, New York, 1969.

[45] A. Demetriades. Transition in high-speed shear layers. In M. Y. Hussaini and R.G. Voigt, editors, *Instability and Transition, Volume I*, pages 52–67, Berlin, 1990. Springer-Verlag.

[46] D. Papamoschou and A. Roshko. The compressible turbulent shear layer: an experimental study. *J. of Fluid Mechanics*, 197:453–477, 1988.

[47] Luigi de Luca, Gennaro Cardone, Dominique Chevalerie, and Alain Fonteneau. Viscous interaction phenomena in hypersonic wedge flow. *AIAA Journal*, 33(12):2293–2299, December 1995.

[48] Eli Reshotko and Anatoli Tumin. Role of transient growth in roughness-induced transition. *AIAA Journal*, 42(4):766–770, April 2004.

[49] Hans W. Liepmann. Investigations on laminar boundary-layer stability and transition on curved boundaries. Wartime Report W-107, NACA, August 1943. NASA STI citation 93R23000.

[50] Rudolph A. King and Kenneth S. Breuer. Acoustic receptivity and evolution of two-dimensional and oblique disturbances in a Blasius boundary layer. *Journal of Fluid Mechanics*, 432:69–90, 2001.

[51] R.W. Wlezien. Measurement of acoustic receptivity. Paper 94-2221, AIAA, June 1994.

[52] A.H. Whitehead, Jr. Flowfield and drag characteristics of several boundary-layer tripping elements in hypersonic flow. Technical Note TN-D-5454, NASA, October 1969.

[53] A.L. Braslow and E. A. Horton. Effects of surface roughness on transition. In *NACA Conference on High-Speed Aerodynamics*, pages 439–450, March 1958. Paper is NASA citation 71N75317, conference is citation 71N75285, NASA-TM-X-67369.

[54] Paul F. Holloway and James R. Sterrett. Effect of controlled surface roughness on boundary-layer transition and heat transfer at Mach numbers of 4.8 and 6.0. Technical Note TN-D-2054, NASA, April 1964.

[55] Raymond M. Hicks and William R. Harper, Jr. A comparison of spherical and triangular boundary-layer trips on a flat plate at supersonic speeds. Technical Memorandum TM-X-2146, NASA, December 1970.

[56] Scott Berry, Aaron Auslender, Arthur D. Dilley, and John Calleja. Hypersonic boundary-layer trip development for Hyper-X. *Journal of Spacecraft and Rockets*, 38(6):853–864, Nov.-Dec. 2001.

[57] Albert L. Braslow. A review of factors affecting boundary-layer transition. TN D-3384, NASA, August 1966.

[58] Albert L. Braslow, Eugene C. Knox, and Elmer A. Horton. Effect of distributed three-dimensional roughness and surface cooling on boundary-layer transition and lateral spread of turbulence at supersonic speeds. TN D-53, NASA, October 1959.

[59] E. Leon Morrisette, David R. Stone, and Allen H. Whitehead, Jr. Boundary-layer tripping with emphasis on hypersonic flows. In C. Sinclair Wells, editor, *Viscous Drag Reduction*, pages 33–51. Plenum Press, New York, 1969.

[60] J.R. Sterrett, E.L. Morrisette, A.H. Whitehead, Jr., and R.M. Hicks. Transition fixing for hypersonic flow. In *Conference on Hypersonic Aircraft Technology*, pages 203–222, May 1967. Paper is NASA citation 74N73064, conference is citation 74N73049, NASA-SP-148.

[61] Albert L. Braslow, Raymond M. Hicks, and Roy V. Harris, Jr. Use of grit-type boundary-layer transition trips on wind-tunnel models. Technical Note TN-D-3579, NASA, September 1966.

[62] E. Leon Morrisette, David R. Stone, and Aubrey M. Cary, Jr. Downstream effects of boundary-layer trips in hypersonic flow. In *Compressible Turbulent Boundary Layers*, pages 437–453. NASA, January 1969. NASA citation 70N10442.

[63] E.R. Van Driest and C.B. Blumer. Summary report on studies on boundary layer transition for years 1963-1964. Technical Report SID 64-2191, North American Aviation, Inc., Space Sciences Laboratory, December 1964. Cited in Morrisette et al. 1969. Not available from any known archive.

[64] Robert Korkegi. Transition studies and skin-friction measurements on an insulated flat plate at a Mach number of 5.8. *J. of the Aeronautical Sciences*, 23(2):97–107 and 192, February 1956.

[65] J.L. Potter and J.D. Whitfield. Effects of unit Reynolds number, nose bluntness, and roughness on boundary layer transition. Technical Report AEDC-TR-60-5, Arnold Engineering Development Center, March 1960.

[66] J.L. Potter and J.D. Whitfield. *Boundary-layer transition under hypersonic conditions*, pages 1–62. AGARD, May 1965. AGARDograph 97, Part III.

[67] W.D. McCauley, A.R. Saydah, and J.F. Bueche. The effect of controlled three-dimensional roughness on hypersonic boundary-layer transition. Paper 66-26, AIAA, January 1966.

[68] W.D. McCauley, A.R. Saydah, and J.F. Bueche. Effect of spherical roughness on hypersonic boundary-layer transition. *AIAA Journal*, 4(12):2142–2148, December 1966.

[69] E.R. Van Driest and J. Christopher Boison. Experiments on boundary-layer transition at supersonic speeds. *Journal of the Aeronautical Sciences*, 24:885–899, December 1957.

[70] John J. Bertin, E.S. Idar III, and Winston D. Goodrich. Effect of surface cooling and roughness on transition for the shuttle orbiter. *J. of Spacecraft and Rockets*, 15(2):113–119, March-April 1978.

[71] Daniel Arnal and Jean Delery. Laminar-turbulent transition and shock wave/boundary-layer interaction. In *Critical technologies for hypersonic vehicle development*. NATO RTO, December 2005. Paper 4 in RTO-EN-AVT-116, 46 pages. NASA STI citation 20060010492.

[72] E.R. Van Driest, C.B. Blumer, and C.S. Wells, Jr. Boundary layer transition on blunt bodies – effects of roughness. *AIAA Journal*, 5:1913–1915, October 1967.

[73] J. Leith Potter and Jack D. Whitfield. Effects of slight nose bluntness and roughness on boundary-layer transition in supersonic flows. *J. of Fluid Mechanics*, 12:501–535, 1961.

[74] Paul F. Holloway and E. Leon Morrisette. Roughness effects on boundary-layer transition for blunt-leading-edge plates at Mach 6. Technical Note TN-D-3517, NASA, August 1966.

[75] M.R. Wool. Interim report, passive nosetip technology (PANT) program, volume X, Summary of experimental and analytical results (for the period May 1973 to December 1974). Technical Report TR-74-86-Vol-X, SAMSO, January 1975. Citation AD-A020708 in DTIC.

[76] Rudolph Swigart. Roughness-induced boundary-layer transition on blunt bodies. *AIAA J.*, 10(10):1355–1356, October 1972.

[77] A.H. Boudreau. Correlation of artificially induced boundary-layer transition data at hypersonic speeds. *Journal of Spacecraft and Rockets*, 18(2):152–156, March-April 1981.

[78] K.F. Stetson. Nosetip bluntness effects on cone frustum boundary layer transition in hypersonic flow. Paper 83-1763, AIAA, July 1983.

[79] Catherine B. McGinley, Scott A. Berry, Gerald R. Kinder, Maria Barnwell, Kuo C. Wang, and Benjamin S. Kirk. Review of orbiter flight boundary layer transition data. Paper 2006-2921, AIAA, June 2006.

[80] Scott A. Berry, H. Harris Hamilton II, and Kathryn E. Wurster. Effect of computational method on discrete roughness correlations for shuttle orbiter. *J. of Spacecraft and Rockets*, 43(4):842–852, July-August 2006.

[81] J.J. Bertin, K.S. Stetson, S. A. Bouslog, and J.M. Caram. Effects of isolated roughness elements on boundary-layer transition for shuttle orbiter. *J. of Spacecraft and Rockets*, 34(4):426–436, July-August 1997.

[82] M.C. Fischer. Spreading of a turbulent disturbance. *AIAA Journal*, 10(7):957–959, 1972.

[83] Brenda M. Kulfan. Reynolds number considerations for supersonic flight. Paper 2002-2839, AIAA, June 2002.

[84] James C. Daugherty and Raymond M. Hicks. Measurements of local skin friction downstream

of grit-type boundary-layer transition trips at Mach 2.17 and zero heat transfer. *AIAA Journal*, 8(5):940–941, May 1970.

[85] John B. Peterson, Jr. Boundary-layer velocity profiles downstream of three-dimensional transition trips on a flat plate at Mach 3 and 4. Technical Note TN-D-5523, NASA, November 1969.

[86] I. Beckwith, F. Chen, S. Wilkinson, M. Malik, and D. Tuttle. Design and operational features of low-disturbance wind tunnels at NASA Langley for Mach numbers from 3.5 to 18. Paper 90-1391, AIAA, June 1990.

[87] Thomas J. Juliano, Erick O. Swanson, and Steven P. Schneider. Transition research and improved performance in the Boeing/AFOSR Mach-6 quiet tunnel. Paper 2007-0535, AIAA, January 2007.

[88] Steven P. Schneider. Fabrication and testing of the Purdue Mach-6 quiet-flow Ludwieg tube. Paper 2000-0295, AIAA, January 2000.

[89] Steven P. Schneider. Design of a Mach-6 quiet-flow wind-tunnel nozzle using the e**N method for transition estimation. Paper 98-0547, AIAA, January 1998.

[90] Jim J. Jones. Experimental investigation of the heat-transfer rate to a series of 20-deg. cones of various surface finishes at a Mach number of 4.95. Technical Memorandum NASA-MEMO-6-10-59L, NASA, June 1959.

[91] Winston D. Goodrich, Stephen M. Derry, and John J. Bertin. Shuttle orbiter boundary layer transition at flight and wind tunnel conditions. In *Shuttle Performance: Lessons Learned*, pages 753–780, March 1983. NASA-CP-2283, Part I.

[92] Winston D. Goodrich, Stephen M. Derry, and John J. Bertin. Shuttle orbiter boundary layer transition: A comparison of flight and wind tunnel data. Paper 83-0485, AIAA, January 1983.

[93] Scott A. Berry, Thomas J. Horvath, Amy M. Cassaday, Benjamin S. Kirk, K.C. Wang, and Andrew J. Hyatt. Boundary layer transition results from STS-114. Paper 2006-2922, AIAA, June 2006.

[94] D.M. Tellep and H. Hoshizaki. X-17 re-entry test vehicle: R-26 final flight report. Technical Report LMSD-2600, Lockheed Aircraft Corp., November 1957. Citation AD802033 in DTIC.

[95] D.I.A. Poll. Laminar-turbulent transition. In William S. Saric, Jean Muylaert, and Christian Dujarric, editors, *Hypersonic Experimental and Computational Capability, Improvement and Validation*, pages 3–1 to 3–20. AGARD, May 1996. AR-319 v. I.